5. Development of vasicine derivatives

5.1. Experimental section

5.1.1. Chemistry

5.1.1.1. General method

All the solvents and chemicals were used from commercial products and further, no purification processing was done. The experiments were carried out under N_2 conditions and oven-dried glassware was used. All the reactions were monitored using precoated silica gel 60 F254 (Merck KGaA, Germany) and TLC plates were observed under an iodine chamber, UV light, and Dragendorff's reagent (visualization of spots for alkaloidal compounds). The melting point of compounds was carried out on melting point apparatus (Stuart SMP10, UK) using capillary tubes. The compounds were characterized using ^{1}H NMR (Bruker Bio spin International AG, Germany), ^{13}C NMR (Bruker Bio spin International AG, Germany), HRMS (SCIEX. X500R QTOF, US), and SC-XRD (Bruker D8 Venture, Germany) was performed at SAIF, IIT Madras. HRMS was carried out at the Department of chemistry, Banaras Hindu University, Varanasi.

The purity of compounds was estimated by HPLC (Waters 1500 series, Germany) and samples were prepared using a 0.45 µm membrane filter for analysis. The concentration of sample 100 µL was prepared in methanol and injection volume was set as 10µL-20µL. In this, Lichro CART 250-4 C_{18} column was used. Mobile phase was selected as, methanol and water (9:1) with a flow rate of 1 mL/min. PDA detector 2998 was used to detect the samples 280 nm wavelength. The resulting data and percentage purity of compounds were analyzed using waters breeze software.

5.1.1.2. Extraction and Isolation of vasicine from *Adhatoda vasica*

The dried powdered leaves of *Adhatoda vasica* (Family: Acanthaceae) were purchased from Vedic vatica private limited, Chhattisgarh, India. In this process, 1 kg of leaves powder was transferred into maceration chamber, and methanol (3 L) was added. This mixture was kept at room temperature and stirred every 4. After 72 h, the mixture was filtered using a muslin cloth/filter paper. The process was repeated 3 times at a time interval of 72 h. The obtained methanolic extract was concentrated under reduced pressure (rotary evaporator). The resulting crude residue was transferred into a petri dish and calculated the yield using formula [Percentage yield = (Weight of obtained crude extract or fraction in grams) – Weight of the plant material grams) / 100].

The obtained semi-solid extract (100 g) was dissolved into water (1L). followed by an aqueous mixture that was treated with hexane (1L) 3 times to remove the chlorophyll and highly nonpolar compound (fatty acids and oils etc.). The obtained aqueous mixture was basified with aqueous ammonia to get a pH of 12-13. The basified solution was further extracted with DCM/chloroform (1L) 3 times. The resulting DCM extract was evaporated under reduced pressure. Next, column was loaded with silica gel (60-120 mesh) and slurry was prepared using hexane (Figure 5.1). The mobile phase used was dichloromethane and methanol by gradually increasing polarity (gradient method). The column started with DCM (100 %) and end with DCM: methanol (95:5). The obtained fractions were monitored by TLC, for this mobile phase used as dichloromethane: methanol (9:1) and stationary phased used as precoated silica gel 60 F254 (Merck KGaA, Germany). The resulting TLC plates were observed by keeping them in an iodine chamber, under UV light, and Dragendorff's reagent for detection of vasicine and its analogs (VA01-VA25).

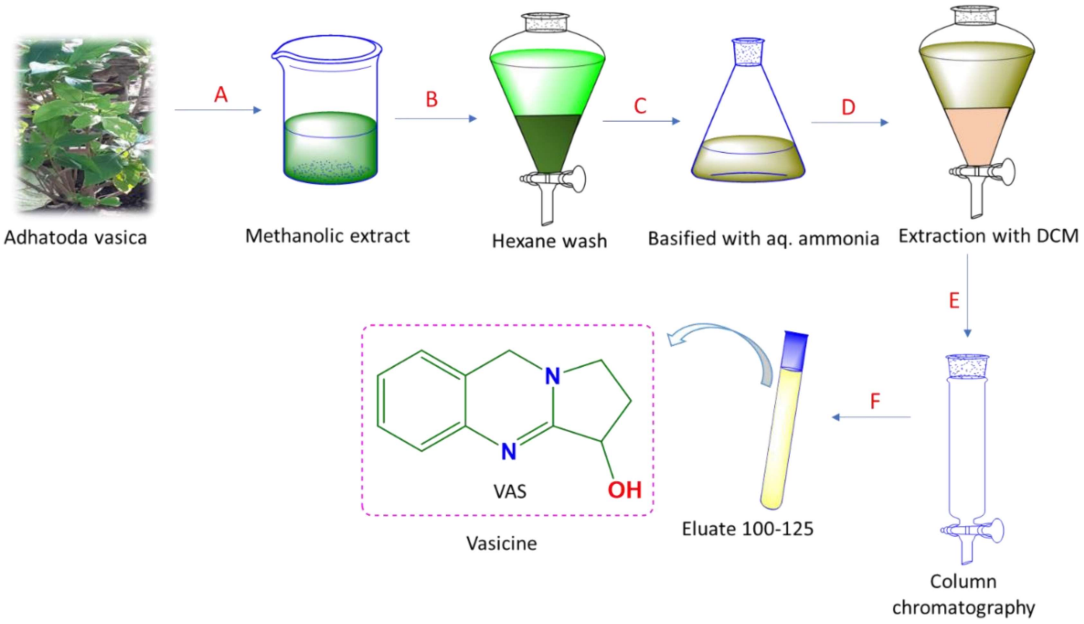

Figure 5.1. Process of isolation of vasicine from *Adhatoda vasica*

1,2,3,9-tetrahydropyrrolo[2,1-b] quinazolin-3-ol (VA): brown solid, M.P-209°C, HPLC purity- 99.98%, ^{1}H NMR (500 MHz, $CDCl_3$) δ 7.20 – 7.14 (m, 2H), 7.02 – 6.97 (m, 1H), 6.89 (d, J = 7.8 Hz, 1H), 4.82 – 4.76 (m, 1H), 4.67 – 4.57 (m, 2H), 3.44 – 3.40 (m, 1H), 3.29 – 3.24 (m, 1H), 2.42 – 2.37 (m, 1H), 2.15 – 2.09 (m, 1H). ^{13}C NMR (125 MHz, $CDCl_3$) δ 163.7, 142.1, 128.5, 125.8, 124.3, 123.7, 118.9, 70.3, 48.3, 47.1, 28.8. HRMS $[M+H]^+$ was calculated as 189.1028 and found to be 189.1000 for $C_{11}H_{13}N_2O$.

5.1.1.3. Procedure for synthesis of VA0

The isolated vasicine (VA) (1 *eq*) was taken into 100 mL RBF and dissolved in water: methanol (1:1) 20 mL. The RBF was placed on magnetic stirrer for stirring at 5-10°C (10 min). Then, $NaBH_4$ (3 *eq*) was added slowly for up to 30 min and reaction was kept at room temperature for 4 hrs. Reaction was monitored by TLC until reaction was completed. The reaction was stopped by quenching ethyl acetate into reaction mixture, followed by washing with water (3×20 mL). Then obtained ethyl acetate fraction was treated with sodium sulfate, filtered, and dried under reduced pressure. The residue was purified by column chromatography using silica

gel (60-120 mesh) and mobile phase [ethyl acetate: methanol (98:2)] to afford the desired compound.

1-(2-aminobenzyl)pyrrolidin-3-ol (VA0): semi-solid, Pale yellow, yield-94 %, ^{1}H NMR (500 MHz, $CDCl_3$) δ 7.10 – 7.07 (m, 1H), 7.00 (dd, J = 7.4, 1.1 Hz, 1H), 6.71 – 6.60 (m, 2H), 4.35 – 4.32 (m, 1H), 3.66 – 3.52 (m, 2H), 2.82 – 2.78 (m, 1H), 2.59 (dd, J = 10.3, 2.1 Hz, 1H), 2.52 (dd, J = 10.3, 5.3 Hz, 1H), 2.32 – 2.27 (m, 1H), 2.20 – 2.12 (m, 1H), 1.74 – 1.68 (m, 1H), 1.43 – 1.20 (m, 2H). ^{13}C NMR (125 MHz, $CDCl_3$) δ 146.5, 129.8, 128.3, 123.4, 117.7, 115.5, 71.4, 62.7, 59.1, 52.3, 34.9.

5.1.1.4. General procedure for synthesis of VA01-VA25

VA0 (1.0 *eq*) was transferred into RBF and dissolved into acetonitrile (5 mL) and reaction temperature was set to room temperature. To this, diisopropylethylamine (DIPEA) (2.5 *eq*) was added followed by addition of carboxylic acids 1-25 (1.2 eq). Then, 1-hydroxy benzotriazole (HOBT) (2.5 *eq*) was added and reaction was cooled to 10°C. Finally, N-(3-Dimethylaminopropyl)-N-ethyl carbodiimide. HCl (1.5 *eq*) was added. The reaction was stirred at room temperature for 6 to 8 hrs. The progress of reaction was monitored by TLC and reaction was stopped by quenching of 20 mL of water. Then the mixture was extracted with dichloromethane (3×10 mL). The obtained residue was purified by column chromatography using silica gel (60-120 mesh) and mobile phase was selected as ethyl acetate: MeOH (95:5) to afford the desired compound.

N-(2-((3-hydroxypyrrolidin-1-yl)methyl)phenyl)benzamide (VA01): light brown solid, yield-97 %, M.P-186°C, ^{1}H NMR (500 MHz, $CDCl_3$) δ 11.64 (s, 1H), 8.43 (d, J = 5.7 Hz, 1H), 8.04 (d, J = 7.3 Hz, 2H), 7.55 – 7.47 (m, 3H), 7.37 (t, J = 7.4 Hz, 1H), 7.17 (d, J = 7.3 Hz, 1H), 7.06 (t, J = 7.3 Hz, 1H), 4.52 (dd, J = 7.2, 5.1 Hz, 1H), 3.82 – 3.76 (m, 2H), 2.95 (d, J = 5.3 Hz, 1H), 2.85 – 2.64 (m, 2H), 2.46 (s, 1H), 2.29 (dd, J = 13.4, 5.9 Hz, 1H), 2.02 – 1.71 (m, 2H). *D_2O*

exchange: ^{1}H NMR (500 MHz, $CDCl_3$) δ 8.45 (d, J = 8.1 Hz, 1H), 8.03 (d, J = 7.3 Hz, 2H), 7.55 – 7.47 (m, 3H), 7.37 (dd, J = 11.3, 4.2 Hz, 1H), 7.16 (d, J = 7.2 Hz, 1H), 7.05 (t, J = 7.4 Hz, 1H), 4.80 (s, 2H), 4.57 – 4.46 (m, 1H), 3.86 – 3.71 (m, 2H), 2.96 – 2.91 (m, 1H), 2.76 – 2.67 (m, 2H), 2.45 (dd, *J* = 15.9, 8.5 Hz, 1H), 2.31 – 2.25 (m, 1H), 1.88 – 1.82 (m, 1H). ^{13}C NMR (125 MHz, $CDCl_3$) δ 165.2, 138.7, 135.2, 131.6 (2C), 129.1, 128.6 (3C), 127.3 (2C), 126.4, 123.4, 71.1, 62.6, 59.5, 52.4, 35.0. HRMS $[M+H]^+$ was calculated as 297.1603 and found to be 297.1578 for $C_{18}H_{21}N_2O_2$.

2-fluoro-N-(2-((3-hydroxypyrrolidin-1-yl)methyl)phenyl)benzamide (VA02): white solid, yield-98 %, M.P-180°C, ^{1}H NMR (500 MHz, $CDCl_3$) δ 11.09 (s, 1H), 8.38 (d, J = 8.1 Hz, 1H), 8.10 (t, J = 7.6 Hz, 1H), 7.51 (d, J = 6.2 Hz, 1H), 7.37 (t, J = 7.7 Hz, 1H), 7.30 (dd, J = 14.0, 6.5 Hz, 1H), 7.18 (dd, J = 12.9, 6.2 Hz, 2H), 7.08 (t, J = 7.4 Hz, 1H), 4.39 (s, 1H), 3.74 (s, 2H), 2.81 (dd, J = 14.7, 8.0 Hz, 1H), 2.68 (dd, J = 10.1, 5.6 Hz, 1H), 2.60 (d, J = 10.1 Hz, 1H), 2.42 (d, J = 6.8 Hz, 1H), 2.21 (dd, J = 14.0, 6.9 Hz, 1H), 1.75 (dd, J = 14.1, 7.6 Hz, 2H). ^{13}C NMR (125 MHz, $CDCl_3$) δ 161.6, 138.0, 133.2, 133.1, 132.0, 129.3, 128.3, 127.5, 124.8 (d, *J* = 3.2 Hz), 124.8, 124.0, 121.9, 116.1, 71.3, 62.4, 59.2, 52.1, 35.0. HRMS $[M+H]^+$ was calculated as 315.1509 and found to be 315.1481 for $C_{18}H_{20}FN_2O_2$.

3-fluoro-N-(2-((3-hydroxypyrrolidin-1-yl)methyl)phenyl)benzamide (VA03): light brown solid, yield-98 %, M.P.- 178°C, ^{1}H NMR (500 MHz, $CDCl_3$) δ 11.75 (s, 1H), 8.42 (d, J = 8.0 Hz, 1H), 7.85 (d, J = 7.7 Hz, 1H), 7.75 (d, J = 12.3 Hz, 1H), 7.48 – 7.44 (m, 1H), 7.37 (t, J = 7.7 Hz, 1H), 7.25 – 7.22 (m, 1H), 7.17 (d, *J* = 7.2 Hz, 1H), 7.07 (t, J = 7.4 Hz, 1H), 4.56 – 4.54 (m, 1H), 3.83 – 3.76 (m, 2H), 2.98 (dd, J = 14.1, 8.5 Hz, 1H), 2.78 (d, J = 10.4 Hz, 1H), 2.68 (dd, J = 10.4, 5.2 Hz, 1H), 2.48 (dd, J = 15.8, 8.4 Hz, 1H), 2.38 – 2.24 (m, 1H), 1.92 – 1.86 (m, 1H), 1.77 (s, 1H). ^{13}C NMR (125 MHz, $CDCl_3$) δ 163.8, 138.5, 130.2 (d, *J* = 7.9 Hz), 130.2, 129.1, 128.5, 126.4, 123.6, 123.0, 120.8, 118.6, 118.4, 114.3, 71.1, 62.5, 59.5, 52.5, 34.9.

4-fluoro-N-(2-((3-hydroxypyrrolidin-1-yl)methyl)phenyl)benzamide (VA04): light brown solid, yield-98 %, M.P-180°C, ^{1}H NMR (500 MHz, $CDCl_3$) δ 11.67 (s, 1H), 8.40 (d, J = 8.1 Hz, 1H), 8.09 – 8.06 (m, 2H), 7.37 – 7.34 (m, 1H), 7.17 – 7.13 (m, 3H), 7.07 – 7.04 (m, 1H), 4.55 – 7.53 (m, 1H), 3.82 – 3.73 (m, 2H), 3.00 – 2.96 (m, 1H), 2.82 (d, J = 10.6 Hz, 1H), 2.63 (dd, J = 10.5, 5.3 Hz, 1H), 2.41 (dd, J = 16.4, 8.3 Hz, 1H), 2.32 – 2.26 (m, 1H), 2.03 (s, 1H), 1.90 – 1.84 (m, 1H). ^{13}C NMR (125 MHz, $CDCl_3$) δ 165.8, 164.1, 138.6, 131.3, 129.8, 129.7 (d, *J* = 8.9 Hz), 129.1, 128.5, 126.4, 123.5, 120.8, 115.6, 115.5, 71.1, 62.6, 59.5, 52.5, 34.9.

2-chloro-N-(2-((3-hydroxypyrrolidin-1-yl)methyl)phenyl)benzamide (VA05): light yellow solid, yield-99 %, M.P-177°C, ^{1}H NMR (500 MHz, $CDCl_3$) δ 11.33 (s, 1H), 8.45 (d, J = 8.1 Hz, 1H), 7.69 (dd, J = 7.2, 1.7 Hz, 1H), 7.48 – 7.46 (m, 1H), 7.42 – 7.36 (m, 3H), 7.15 (d, J = 7.3 Hz, 1H), 7.07 (t, J = 7.4 Hz, 1H), 4.30 (dd, J = 7.0, 5.2 Hz, 1H), 3.85 – 3.79 (m, 1H), 3.72 (d, J = 13.2 Hz, 1H), 2.84 – 2.73 (m, 1H), 2.65 (dd, J = 10.6, 5.2 Hz, 1H), 2.58 (d, J = 10.3 Hz, 1H), 2.37 (dd, J = 15.2, 8.7 Hz, 1H), 2.12 – 2.01 (m, 2H), 1.66 – 1.60 (m, 1H). ^{13}C NMR (125 MHz, $CDCl_3$) δ 164.7, 138.3, 136.7, 131.1, 130.6, 130.2, 129.6, 129.1, 128.5, 127.1, 126.4, 123.8, 120.8, 71.1, 62.3, 59.2, 51.9, 34.9.

3-chloro-N-(2-((3-hydroxypyrrolidin-1-yl)methyl)phenyl)benzamide (VA06): light yellow solid, yield-98 %, M.P-181°C,^{1}H NMR (500 MHz, $CDCl_3$) δ 11.83 (s, 1H), 8.35 (d, *J* = 7.9 Hz, 1H), 8.06 – 7.77 (m, 2H), 7.50 – 7.27 (m, 3H), 7.20 – 6.95 (m, 2H), 4.50 (d, *J* = 2.8 Hz, 1H), 3.83 – 3.66 (m, 2H), 2.92 (dd, *J* = 14.3, 7.7 Hz, 1H), 2.68 (s, 1H), 2.52 – 2.49 (m, 1H), 2.29 – 2.22 (m, 1H), 2.16 (s, 1H), 2.03 (t, *J* = 11.8 Hz, 1H), 1.91 – 1.88 (m, 1H). ^{13}C NMR (125 MHz, $CDCl_3$) δ 163.7, 138.4, 136.9, 134.6, 131.5, 130.0, 129.1, 128.4, 127.2, 126.6, 125.7, 123.7, 120.8, 70.9, 62.2, 59.5, 52.5, 34.8.

4-chloro-N-(2-((3-hydroxypyrrolidin-1-yl)methyl)phenyl)benzamide (VA07): light yellow solid, yield-99 %, M.P-186°C, ^{1}H NMR (500 MHz, $CDCl_3$) δ 11.73 (s, 1H), 8.41 (d, J = 8.2

Hz, 1H), 7.99 (dd, J = 21.9, 10.0 Hz, 2H), 7.45 (d, J = 8.5 Hz, 2H), 7.36 (t, J = 7.8 Hz, 1H), 7.16 (d, J = 7.4 Hz, 1H), 7.06 (t, J = 7.4 Hz, 1H), 4.55 – 4.53 (m, 1H), 3.82 – 3.73 (m, 2H), 3.00 – 2.95 (m, 1H), 2.81 (d, J = 10.6 Hz, 1H), 2.62 (dd, J = 10.6, 5.4 Hz, 1H), 2.40 (dd, J = 16.5, 8.5 Hz, 1H), 2.33 – 2.26 (m, 1H), 2.01 (s, 1H), 1.90 – 1.84 (m, 1H). ^{13}C NMR (125 MHz, $CDCl_3$) δ 164.1, 138.6, 137.8, 133.5, 129.1, 128.8 (4C), 128.5, 126.4, 123.5, 120.8, 71.1, 62.6, 59.6, 52.5, 34.9. HRMS $[M+H]^+$ was calculated as 331.1213 and found to be 331.1273 for $C_{18}H_{20}ClN_2O_2$.

2-bromo-N-(2-((3-hydroxypyrrolidin-1-yl)methyl)phenyl)benzamide (VA08): light orange solid, yield-96 %, M.P-173°C, ^{1}H NMR (500 MHz, $CDCl_3$) δ 11.60 (s, 1H), 8.47 – 8.22 (m, 1H), 7.56 (d, J = 7.4 Hz, 2H), 7.41 – 7.29 (m, 2H), 7.14 (d, J = 7.2 Hz, 1H), 7.04 (d, J = 6.9 Hz, 2H), 4.47 (d, J = 3.2 Hz, 1H), 3.85 (s, 2H), 3.75 (s, 1H), 2.96 – 2.87 (m, 1H), 2.71 (s, 1H), 2.50 (s, 1H), 2.27 – 2.20 (m, 1H), 2.03 (t, J = 11.9 Hz, 1H), 1.90 – 1.80 (m, 1H). ^{13}C NMR (125 MHz, $CDCl_3$) δ 165.2, 159.8, 138.5, 136.5, 129.6, 129.3, 128.5, 126.6, 123.7, 119.2, 117.2, 113.1, 70.9, 62.4, 59.3, 55.5, 52.4, 34.8.

3-bromo-N-(2-((3-hydroxypyrrolidin-1-yl)methyl)phenyl)benzamide (VA09): light orange solid, yield-94 %, M.P-161°C, ^{1}H NMR (500 MHz, $CDCl_3$) δ 11.81 (s, 1H), 8.33 (d, J = 6.6 Hz, 1H), 8.10 (s, 1H), 7.98 (d, J = 6.4 Hz, 1H), 7.61 (d, J = 6.5 Hz, 1H), 7.32 (s, 2H), 7.15 (d, J = 5.8 Hz, 1H), 7.05 (s, 1H), 4.52 (s, 1H), 3.85 (d, J = 12.7 Hz, 1H), 3.70 (d, J = 12.8 Hz, 1H), 2.96 (t, J = 17.9 Hz, 1H), 2.70 (s, 2H), 2.54 (s, 1H), 2.26 (d, J = 6.0 Hz, 1H), 1.91 (s, 1H), 1.31 (d, J = 4.6 Hz, 1H). ^{13}C NMR (125 MHz, $CDCl_3$) δ 163.7, 138.4, 137.1, 134.5, 130.3, 130.0, 129.2, 128.5, 126.6, 126.3, 123.8, 122.6, 121.1, 70.9, 62.2, 59.4, 52.5, 34.8.

4-bromo-N-(2-((3-hydroxypyrrolidin-1-yl)methyl)phenyl)benzamide (VA10): orange solid, yield-97 %, M.P-179°C, HPLC purity-97.88%, ^{1}H NMR (500 MHz, $CDCl_3$) δ 11.75 (s, 1H), 8.40 (d, J = 8.1 Hz, 1H), 8.00 – 7.87 (m, 2H), 7.67 – 7.55 (m, 2H), 7.40 – 7.31 (m, 1H), 7.20 –

7.11 (m, 1H), 7.07 – 7.04 (m, 1H), 4.56 – 4.53 (m, 1H), 3.85 – 3.68 (m, 2H), 3.00 – 2.96 (m, 1H), 2.81 (d, J = 10.6 Hz, 1H), 2.62 (dd, J = 10.7, 5.4 Hz, 1H), 2.40 (dd, J = 16.4, 8.6 Hz, 1H), 2.34 – 2.25 (m, 1H), 1.89 – 1.83 (m, 1H), 1.79 (s, 1H). ^{13}C NMR (125 MHz, $CDCl_3$) δ 164.2, 138.5, 134.0, 131.8 (2C), 129.1, 129.0 (2C), 128.5, 126.4, 126.3, 123.6, 120.8, 71.1, 62.6, 59.6, 52.5, 34.9. HRMS $[M+H]^+$ was calculated as 375.0708 and found to be 375.0672 for $C_{18}H_{20}BrN_2O_2$.

N-(2-((3-hydroxypyrrolidin-1-yl)methyl)phenyl)-2-iodobenzamide (VA11): white solid, yield-99 %, M.P-175°C, ^{1}H NMR (500 MHz, $CDCl_3$) δ 11.39 (s, 1H), 8.45 (d, J = 8.1 Hz, 1H), 7.98 – 7.90 (m, 1H), 7.55 (dd, J = 7.6, 1.5 Hz, 1H), 7.45 – 7.42 (m, 1H), 7.39 – 7.36 (m, 1H), 7.16 – 7.13 (m, 2H), 7.09 – 7.06 (m, 1H), 4.28 (d, J = 2.1 Hz, 1H), 3.85 (d, J = 13.3 Hz, 1H), 3.73 (d, J = 13.3 Hz, 1H), 2.82 – 2.78 (m, 1H), 2.64 – 2.57 (m, 2H), 2.35 (dd, J = 15.3, 8.7 Hz, 1H), 2.10 – 2.03 (m, 1H), 1.71 (s, 1H), 1.64 – 1.59 (m, 1H). ^{13}C NMR (126 MHz, $CDCl_3$) δ 167.1, 142.9, 140.1, 138.4, 131.1, 129.0, 128.5, 128.2, 128.1, 126.2, 123.8, 120.5, 92.4, 71.1, 62.3, 59.2, 51.9, 34.9. HRMS $[M+H]^+$ was calculated as 423.0569 and found to be 423.0548 for $C_{18}H_{20}IN_2O_2$.

3-cyano-N-(2-((3-hydroxypyrrolidin-1-yl)methyl)phenyl)benzamide (VA12): white solid, yield-98 %, M.P-170°C, ^{1}H NMR (500 MHz, $CDCl_3$) δ 12.03 (s, 1H), 8.44 (s, 1H), 8.38 (t, *J* = 9.1 Hz, 2H), 7.81 (d, *J* = 7.7 Hz, 1H), 7.63 (t, *J* = 7.8 Hz, 1H), 7.42 – 7.32 (m, 1H), 7.18 (d, *J* = 7.1 Hz, 1H), 7.08 (t, *J* = 7.1 Hz, 1H), 4.59 (t, *J* = 5.7 Hz, 1H), 3.84 (d, *J* = 13.3 Hz, 1H), 3.75 (d, *J* = 13.2 Hz, 1H), 3.11 – 3.02 (m, 1H), 2.89 (d, *J* = 10.6 Hz, 1H), 2.54 (dd, *J* = 10.4, 4.8 Hz, 1H), 2.44 – 2.28 (m, 2H), 2.01 – 1.91 (m, 1H), 1.75 (s, 1H). ^{13}C NMR (125 MHz, $CDCl_3$) δ 162.8, 138.3, 136.3, 134.6, 132.4, 130.8, 129.6, 129.1, 128.5, 126.5, 123.9, 120.9, 118.6, 112.7, 71.1, 62.3, 59.6, 52.5, 34.8. HRMS $[M+H]^+$ was calculated as 322.1556 and found to be 322.1609 for $C_{19}H_{20}N_3O_2$.

N-(2-((3-hydroxypyrrolidin-1-yl)methyl)phenyl)-2-nitrobenzamide (VA13): brown solid, yield-94 %, M.P-200°C, ^{1}H NMR (500 MHz, $CDCl_3$) δ 11.77 (s, 1H), 8.30 (d, J = 8.0 Hz, 1H), 7.92 (d, J = 8.0 Hz, 1H), 7.72 (d, J = 7.4 Hz, 1H), 7.65 (t, J = 7.4 Hz, 1H), 7.53 (t, J = 7.6 Hz, 1H), 7.29 (t, J = 7.5 Hz, 1H), 7.09 (d, J = 7.2 Hz, 1H), 7.03 (t, J = 7.3 Hz, 1H), 4.19 (d, J = 2.7 Hz, 1H), 3.72 – 3.65 3.68 (m, 2H), 3.08 (dd, J = 15.9, 6.3 Hz, 1H), 2.69 (dd, J = 14.3, 8.0 Hz, 1H), 2.45 (s, 1H), 2.28 – 2.24 (m, 1H), 1.95 – 1.88 (m, 1H), 1.53 (dd, J = 12.9, 6.6 Hz, 1H), 1.10 – 0.97 (m, 1H). ^{13}C NMR (125 MHz, $CDCl_3$) δ 163.9, 147.1, 138.2, 133.6, 132.9, 130.7, 129.1, 128.3, 126.6, 124.3, 124.0, 120.6, 70.4, 61.9, 59.1, 52.0, 45.1, 34.5.

N-(2-((3-hydroxypyrrolidin-1-yl)methyl)phenyl)-3-nitrobenzamide (VA14): brown solid, yield-98 %, M.P-190°C, ^{1}H NMR (500 MHz, $CDCl_3$) δ 12.04 (s, 1H), 8.79 (s, 1H), 8.49 (d, J = 7.8 Hz, 1H), 8.46 – 8.36 (m, 2H), 7.71 (t, J = 8.0 Hz, 1H), 7.39 (dd, J = 11.4, 4.2 Hz, 1H), 7.20 (d, J = 7.2 Hz, 1H), 7.10 (t, J = 7.4 Hz, 1H), 4.56 (dd, J = 6.8, 5.0 Hz, 1H), 3.92 (d, J = 13.2 Hz, 1H), 3.77 (d, J = 13.2 Hz, 1H), 3.09 – 2.99 (m, 1H), 2.79 (d, J = 10.5 Hz, 1H), 2.71 (dd, J = 10.2, 4.9 Hz, 1H), 2.53 (d, J = 7.0 Hz, 1H), 2.37 – 2.25 (m, 1H), 2.04 (t, J = 12.6 Hz, 1H), 1.93 – 1.88 (m, 1H). ^{13}C NMR (125 MHz, $CDCl_3$) δ 162.5, 148.3, 138.2, 136.9, 134.2, 129.9, 129.1, 128.5, 126.7, 126.1, 124.0, 121.6, 121.0, 71.1, 62.3, 59.7, 52.4, 34.8.

N-(2-((3-hydroxypyrrolidin-1-yl)methyl)phenyl)-4-nitro benzamide (VA15): brown solid, yield-98 %, M.P-206°C,^{1}H NMR (500 MHz, $CDCl_3$) δ 12.14 (s, 1H), 8.33 (s, 1H), 8.25 (s, 4H), 7.32 (t, *J* = 7.1 Hz, 1H), 7.16 (d, *J* = 6.7 Hz, 1H), 7.06 (t, *J* = 6.7 Hz, 1H), 4.55 (s, 1H), 3.80 – 3.73 (m, 2H), 3.01 (s, 1H), 2.85 (t, *J* = 34.7 Hz, 2H), 2.53 (s, 1H), 2.39 – 2.24 (m, 2H), 1.90 (d, *J* = 5.6 Hz, 1H). ^{13}C NMR (125 MHz, $CDCl_3$) δ 163.0, 149.5, 140.5, 138.1, 129.2, 128.7, 128.4, 126.6, 124.16, 123.8 (3C), 120.7, 70.9, 62.6, 59.4, 52.5, 34.8. HRMS $[M+H]^+$ was calculated as 342.1454 and found to be 342.1505 for $C_{18}H_{20}N_3O_4$.

N-(2-((3-hydroxypyrrolidin-1-yl)methyl)phenyl)-3-methoxybenzamide (VA16): pale yellow solid, yield-97 %, M.P-169°C, ^{1}H NMR (500 MHz, $CDCl_3$) δ 11.40 (s, 1H), 8.38 (d, *J* = 8.0 Hz, 1H), 7.59 (dd, *J* = 17.3, 7.7 Hz, 2H), 7.40 – 7.30 (m, 2H), 7.27 (dd, *J* = 11.8, 4.1 Hz, 1H), 7.12 (d, *J* = 7.2 Hz, 1H), 7.05 (t, *J* = 7.4 Hz, 1H), 4.23 (s, 1H), 3.74 (dd, *J* = 29.3, 12.8 Hz, 2H), 2.72 (dd, *J* = 15.4, 7.8 Hz, 1H), 2.65 – 2.60 (m, 1H), 2.49 (d, *J* = 10.1 Hz, 1H), 2.41 – 2.35 (m, 1H), 2.16 (s, 2H), 2.11 – 1.82 (m, 3H), 1.58 (dd, *J* = 7.6, 5.8 Hz, 1H). ^{13}C NMR (125 MHz, $CDCl_3$) δ 165.8, 138.8, 138.2, 133.4, 131.2, 129.2, 129.1, 128.4, 127.6, 126.5, 123.9, 120.8, 119.2, 70.8, 62.1, 59.1, 51.9, 34.7, 30.9.

N-(2-((3-hydroxypyrrolidin-1-yl)methyl)phenyl)-4-methoxybenzamide (VA17): pale yellow solid, yield-99 %, M.P-172°C, ^{1}H NMR (500 MHz, $CDCl_3$) δ 11.49 (s, 1H), 8.41 (d, *J* = 7.7 Hz, 1H), 8.00 (d, *J* = 8.7 Hz, 2H), 7.35 (t, *J* = 7.7 Hz, 1H), 7.16 (t, *J* = 7.9 Hz, 1H), 7.03 (t, *J* = 7.4 Hz, 1H), 6.97 (d, *J* = 8.6 Hz, 2H), 4.55 – 4.52 (m, 1H), 3.87 (s, 2H), 3.82 – 3.73 (m, 2H), 2.96 (dd, *J* = 13.8, 8.3 Hz, 1H), 2.78 (d, *J* = 10.4 Hz, 1H), 2.74 – 2.64 (m, 1H), 2.45 (d, *J* = 6.4 Hz, 1H), 2.29 (dd, *J* = 13.5, 5.7 Hz, 1H), 2.25 – 2.13 (m, 1H), 2.06 (d, *J* = 9.7 Hz, 1H), 1.89 – 1.86 (m, 1H). ^{13}C NMR (125 MHz, $CDCl_3$) δ 164.9, 162.3, 138.9, 129.1 (3C), 128.5, 127.5, 126.3, 123.2, 113.8 (3C), 71.1, 62.6, 59.6, 55.4, 52.4, 35.0.

N-(2-((3-hydroxypyrrolidin-1-yl)methyl)phenyl)-4-(trifluoromethyl)benzamide (VA18): white solid, yield-97%, M.P-168°C, ^{1}H NMR (500 MHz, $CDCl_3$) δ 11.89 (s, 1H), 8.42 (d, *J* = 8.1 Hz, 1H), 8.20 (d, *J* = 8.1 Hz, 2H), 7.75 (d, *J* = 8.2 Hz, 2H), 7.42 – 7.32 (m, 1H), 7.18 (d, *J* = 6.9 Hz, 1H), 7.09 – 7.06 (m, 1H), 4.58 – 4.55 (m, 1H), 3.79 (dd, *J* = 22.3, 13.0 Hz, 2H), 3.07 – 2.95 (m, 1H), 2.85 (d, *J* = 10.6 Hz, 1H), 2.68 – 2.59 (m, 1H), 2.45 – 2.36 (m, 1H), 2.34 – 2.27 (m, 1H), 2.19 (s, 1H), 1.90 (dd, *J* = 12.3, 6.7 Hz, 1H). ^{13}C NMR (125 MHz, $CDCl_3$) δ 163.7, 138.4, 129.1, 128.5, 127.9 (4C), 126.5, 125.6 (2C), 123.8, 71.1, 62.6, 59.5, 52.5, 50.8, 34.9, 30.9.

N-(2-((3-hydroxypyrrolidin-1-yl)methyl)phenyl)-4-(trifluoromethoxy)benzamide (VA19): yellow solid, yield-98 %, M.P-170°C,^{1}H NMR (500 MHz, $CDCl_3$) δ 11.77 (s, 1H), 8.41 (d, *J* = 8.0 Hz, 1H), 8.13 (d, *J* = 8.6 Hz, 2H), 7.38 – 7.29 (m, 3H), 7.17 (d, *J* = 7.2 Hz, 1H), 7.06 (t, *J* = 7.3 Hz, 1H), 4.56 (s, 1H), 3.78 (dd, *J* = 30.5, 13.1 Hz, 2H), 3.00 (dd, *J* = 12.8, 8.6 Hz, 1H), 2.84 (d, *J* = 10.5 Hz, 1H), 2.62 (dd, *J* = 10.4, 5.1 Hz, 1H), 2.44 – 2.26 (m, 2H), 1.93 – 1.80 (m, 2H). ^{13}C NMR (125 MHz, $CDCl_3$) δ 163.7, 151.5, 138.5, 133.5, 129.3 (3C), 129.1, 128.5, 126.4, 123.6, 120.8, 120.5 (2C), 71.1, 62.6, 59.6, 52.5, 34.9.

4-amino-N-(2-((3-hydroxypyrrolidin-1-yl)methyl)phenyl)benzamide (VA20): white solid, yield-99 %, M.P-183°C, ^{1}H NMR (500 MHz, $CDCl_3$) δ 11.38 (s, 1H), 8.40 (d, *J* = 8.2 Hz, 1H), 7.84 (d, *J* = 8.4 Hz, 2H), 7.33 (t, *J* = 7.3 Hz, 1H), 7.14 (d, *J* = 7.3 Hz, 1H), 7.01 (t, *J* = 7.3 Hz, 1H), 6.69 (d, *J* = 8.6 Hz, 2H), 4.76 (s, 2H), 4.52 – 4.48 (m, 1H), 4.03 (s, 1H), 3.74 (dd, *J* = 34.8, 13.0 Hz, 2H), 3.49 (s, 1H), 2.95 – 2.89 (m, 1H), 2.69 (dd, *J* = 18.8, 13.4 Hz, 1H), 2.43 (dd, *J* = 16.1, 8.4 Hz, 1H), 2.30 – 2.23 (m, 1H), 1.87 – 1.81 (m, 1H). ^{13}C NMR (125 MHz, $CDCl_3$) δ 165.2, 149.7, 139.0, 129.1 (2C), 129.0, 128.4, 126.3, 124.7, 122.9, 120.7, 114.2 (2C), 71.1, 62.6, 59.6, 52.4, 34.9. HRMS $[M+H]^+$ was calculated as 312.1712 and found to be 312.1684 for $C_{18}H_{22}N_3O_2$.

2,4-dichloro-N-(2-((3-hydroxypyrrolidin-1-yl)methyl)phenyl)benzamide (VA21): white solid, yield-99 %, M.P-189°C, ^{1}H NMR (500 MHz, $CDCl_3$) δ 11.38 (s, 1H), 8.42 (d, *J* = 7.5 Hz, 1H), 7.66 (d, *J* = 8.3 Hz, 1H), 7.49 (d, *J* = 2.0 Hz, 1H), 7.44 – 7.32 (m, 2H), 7.16 (d, *J* = 7.2 Hz, 1H), 7.08 (s, 1H), 4.35 (s, 1H), 3.80 (d, *J* = 27.5 Hz, 2H), 2.80 (d, *J* = 5.6 Hz, 1H), 2.61 (dd, *J* = 24.4, 6.9 Hz, 2H), 2.39 (d, *J* = 6.5 Hz, 1H), 2.10 (dd, *J* = 13.8, 6.4 Hz, 1H), 1.70 – 1.63 (m, 2H). ^{13}C NMR (125 MHz, $CDCl_3$) δ 163.7, 138.1, 136.5, 134.9, 131.7, 130.7, 130.1, 129.1, 128.5, 127.4, 126.4, 124.0, 120.8, 71.0, 62.2, 59.2, 52.0, 34.8. HRMS $[M+H]^+$ was calculated as 365.0824 and found to be 365.0883 for $C_{18}H_{19}Cl_2N_2O_2$.

N-(2-((3-hydroxypyrrolidin-1-yl)methyl)phenyl)-3,5-dimethoxybenzamide (VA22): pale yellow, yield-96 %, M.P-160°C, ^{1}H NMR (500 MHz, $CDCl_3$) δ 11.33 (s, 1H), 8.14 (d, *J* = 8.0 Hz, 1H), 7.61 (d, *J* = 2.1 Hz, 1H), 7.59 – 7.55 (m, 1H), 7.33 – 7.28 (m, 1H), 7.16 (d, *J* = 6.5 Hz, 1H), 7.04 – 7.01 (m, 1H), 6.80 (d, *J* = 8.4 Hz, 1H), 4.46 (dd, *J* = 6.9, 4.9 Hz, 1H), 3.89 – 3.80 (m, 9H), 3.01 (dd, *J* = 16.1, 7.7 Hz, 1H), 2.88 – 2.72 (m, 2H), 2.64 – 2.55 (m, 1H), 2.23 – 2.16 (m, 1H), 1.90 – 1.84 (m, 1H). ^{13}C NMR (126 MHz, $CDCl_3$) δ 165.4, 151.9, 148.9, 138.5, 129.7, 128.8, 127.4, 126.7, 124.9, 124.1, 120.0, 111.2, 110.3, 70.5, 62.2, 58.9, 56.0, 55.9, 52.5, 34.5.

N-(2-((3-hydroxypyrrolidin-1-yl)methyl)phenyl)-3,5-dinitrobenzamide (VA23): light brown, yield-97 %, M.P-220°C, ^{1}H NMR (500 MHz, CDCl3) δ 12.42 (s, 1H), 9.35 – 9.09 (m, 3H), 8.40 (s, 1H), 7.41 (t, J = 7.5 Hz, 1H), 7.22 (d, J = 6.5 Hz, 1H), 7.15 (d, J = 6.8 Hz, 1H), 4.54 (s, 1H), 4.04 (d, J = 13.0 Hz, 1H), 3.88 – 3.72 (m, 1H), 3.17 (s, 1H), 2.86 (d, J = 32.2 Hz, 1H), 2.59 (d, J = 41.3 Hz, 2H), 2.37 – 2.24 (m, 1H), 2.00 – 1.92 (m, 1H), 1.78 (s, 1H). ^{13}C NMR (125 MHz, $CDCl_3$) δ 160.3, 148.6 (2C), 138.8, 137.7, 129.2, 128.6, 127.5 (2C), 126.6, 124.6, 121.0 (2C), 70.9, 61.9, 59.5, 52.4, 34.6.

N-(2-((3-hydroxypyrrolidin-1-yl)methyl)phenyl)benzo[d][1,3]dioxole-5-carboxamide (VA24): light brown, yield-96 %, M.P-191°C, ^{1}H NMR (500 MHz, $CDCl_3$) δ 11.51 (s, 1H), 8.37 (s, 1H), 7.61 (d, *J* = 40.7 Hz, 2H), 7.36 (t, *J* = 7.3 Hz, 1H), 7.16 (s, 1H), 7.06 (s, 1H), 6.89 (d, *J* = 8.1 Hz, 1H), 6.05 (s, 2H), 4.54 (dd, *J* = 6.9, 5.1 Hz, 1H), 3.80 (d, *J* = 12.2 Hz, 2H), 2.99 (d, *J* = 15.3 Hz, 1H), 2.82 (s, 1H), 2.67 (s, 1H), 2.45 (s, 1H), 2.31 (dd, *J* = 13.3, 6.1 Hz, 1H), 1.90 (s, 2H). ^{13}C NMR (125 MHz, $CDCl_3$) δ 164.3, 150.4, 148.0 (2C), 138.7, 126.3, 122.4, 108.1 (3C), 107.7, 101.7 (3C), 71.0, 62.6, 52.5 (2C), 34.8. HRMS $[M+H]^+$ was calculated as 341.1501 and found to be 341.1562 for $C_{19}H_{21}N_2O_4$.

(Z)-N-(2-((3-hydroxypyrrolidin-1-yl)methyl)phenyl)-3-phenylacrylamide (VA25): pale yellow, yield-97 %, M.P-176°C, ^{1}H NMR (500 MHz, $CDCl_3$) δ 11.48 (s, 1H), 8.40 (d, *J* = 7.6 Hz, 1H), 7.69 (d, *J* = 15.7 Hz, 1H), 7.56 (d, *J* = 6.5 Hz, 2H), 7.40 – 7.30 (m, 4H), 7.12 (d, *J* = 7.2 Hz, 1H), 7.02 (t, *J* = 7.3 Hz, 1H), 6.66 (d, *J* = 15.7 Hz, 1H), 4.53 (s, 1H), 3.87 (d, *J* = 13.3 Hz, 1H), 3.70 (d, *J* = 13.3 Hz, 1H), 3.01 – 2.97 (m, 1H), 2.85 (d, *J* = 10.3 Hz, 1H), 2.63 (dd, *J* = 10.2, 4.6 Hz, 1H), 2.38 (dd, *J* = 15.5, 8.1 Hz, 1H), 2.32 – 2.24 (m, 2H), 1.91 – 1.86 (m, 1H). ^{13}C NMR (125 MHz, $CDCl_3$) δ 164.3, 140.6, 138.9, 135.0, 129.6, 128.9, 128.8 (2C), 128.3, 127.8 (2C), 125.9, 123.3, 122.8, 120.7, 71.1, 62.4, 59.0, 51.8, 34.9. HRMS $[M+H]^+$ was calculated as 323.1760 and found to be 323.1809 for $C_{20}H_{23}N_2O_2$.

5.1.2. *In silico* studies

5.1.2.1. Molecular docking studies on cholinesterases (AChE and BuChE)

The crystal structure of recombinant human acetylcholinesterase complexed with donepezil (PDB ID: 4EY7) [186] and human butyrylcholinesterase complexed with tacrine (PDB ID: 4BDS) [187] was downloaded from the protein data bank (PDB) site (https://www.rcsb.org/) [188]. Preparation of protein structures, discovery Studio 2021 client version [189] was used. Energy minimization of protein was done using an Amber module that includes, NMR refinement, molecular dynamics, and energy minimization. The 2D structure of ligands was drawn on Chem 3D 20.1.1 software and ligand energies were minimized to optimize the bond length and bond angle.

After completion of above sequential steps, Auto dock 4 software [190] was used for docking studies. The above prepared PDB files (proteins and ligands) were imported into auto dock and saved into pdbqt file format. Further, grid parameters were fixed by targeting amino acids from the active sites; AChE Chain A: Phe295, Trp86, Trp286, Tyr341, Tyr72, Trp286, Tyr337,

Phe338, Tyr341, and BuChE Chain A: Trp82, Ala328, Tha701. The grid size (X:50, Y:48, Z:64) and grid position (X: -15.376, Y: -43.230 Y: 26.903) were validated for AChE. Similarly, BuChE, gride size (X:52, Y:40, Z:56) and grid position (X:132.384, Y:110.549, Z:41.454) were validated. Genetic Algorithms were set to 100 runs and docking parameters were marked as defaults followed by docking assigned through Lamarckian genetic algorithm 4.2. Further, ligands were docked against the target proteins (AChE and BuChE). The resulting docking conformations were seen under the analysis window. These docking conformations (2D and 3D) were analyzed and documented using discovery studio visualizer 2021 client.

5.1.2.2. Molecular Dynamic simulations of VA10

The molecular dynamics studies were performed using Desmond (Maestro-Desmond) software tool [191]. The binding interaction profile and stability of the docked ligands were analyzed on the recombinant human AChE active site (PDB ID: 4EY7) [186]. The studies were carried out using amber 18 of the pmemd module. The refined system was solvated in a cubic box containing TIP3P water molecules to form an aqueous environment and 0.15 M NaCl was added to mimic the ionic strength inside the cell in physiological conditions. The run was performed at a temperature of 310 K and 1 bar at constant volume and temperature (NPT ensemble) under periodic boundary conditions. Before the MD simulation was run, the system was relaxed. Following the MD simulations executed at 100 ns, the results were evaluated via RMSD and RMSF interactions. RMSD plots for the Cα atoms were generated for the protein and ligand-bound protein for each compound to understand the relative stability of the ligand inside its binding pocket using Maestro (Schrödinger, LLC, New York).

5.1.2.3 Drug-likeness, ADME, and toxicity predictions

The drug-likeness, ADME, and toxicity properties of all synthesized compounds were predicted using online software tools swissADME (http://www.swissadme.ch/) [192] and preADMET [193] (https://preadmet.qsarhub.com/).

5.1.3. *In vitro* studies

5.1.3.1. Free-radical scavenging assay

The antioxidant activity of compounds was estimated through DPPH assay [194]. In this assay, DPPH gets reduced in the presence of antioxidant compounds and it produces yellow colour of diphenyl picrylhydrazine. All test samples were prepared in methanol and a total of six different concentrations (200, 100, 50, 30, 20, and 10 µM) were prepared. 75 µL of samples in various concentrations were added into 96-well plates. Followed by, 75 µL of DPPH (100µM final concentration) was added. The samples were incubated at 37° C for 25 min and absorbance was measured at 520 nm wavelength using a microplate reader (SpectraMax M5, US). The reducing capacity of DPPH was calculated using the equation, reducing percentage = [(absorbance of control) - (absorbance of the test)/ (absorbance of control)] × 100. Ascorbic acid (AA) served as a reference compound.

5.1.3.2. Cholinesterase inhibition assay

Cholinesterase (eeAChE/hAChE and eqBuChE) inhibitory activity of compounds was evaluated spectrometrically using reported procedures [195]. These enzymes (eeAChE/hAChE and eqBuChE) were purchased from Sigma Aldrich, USA. The test compounds stock solutions (1 mg/mL) were prepared by dissolving compounds into biological grade dimethyl sulfoxide (DMSO). Further dilutions were made using PBS buffer 7.4. A total of six different concentrations (0.01, 0.1, 1.0, 10, 20, and 40 µM) of sample 2 µL (VA01-VA25) were used to

determine the IC_{50}. The final assay volume consists of 100 µL DTNB (0.0005M), 50 µL of eeAChE/hAChE (0.5 U mL^{-1}), or 50 µL of eqBuChE (0.5 U mL^{-1}) and substrate ATCI (for eeAChE 0.0037 M, 20 µL) or BTCI (for eqBuChE 0.0037 M, 20 µL) was used.

The DTNB was incubated with or without test samples for 10 min in 96-well plates. Followed by, addition of target enzyme (eeAChE/hAChE or eqBuChE). The substrate (ATCI or BTCI) was added after 30 min to this 96-well plate. Yellow colour (5-thio-2-nitrobenzoate anion) was observed by adding DTNB and immediate absorbance was measured at 415 nm, on SpectraMax M5 multi-mode microplate reader. Blank readings were noted, using 2 µL of DMSO instead of test samples. The IC_{50} values of all tested samples were calculated using a log concentration percentage inhibition curve (Graph pad prism 5).

5.1.3.3. Propidium iodide displacement assay

The displacement of propidium iodide assay was carried out to estimate the binding mode at PAS site of AChE inhibitor VA10 [194,196]. A solution of eeAChE 5.0 U/ml was incubated with or without test compounds (5, 10, and 20 µM, 150 µL) for 6hr. at room temperature (24°C). Followed by, addition of propidium iodide (final volume consists of 20 µM) and incubated for 20min. The fluorescence intensity was measured at 535 nm (excitation) and 595 nm (emission) using a microplate reader (SpectraMax M5, US). The percentage inhibition was calculated using formula: $100-(IF_i/IF_0 \times 100)$; where IF_i and IF_0 are fluorescence intensities with and without inhibitors respectively.

5.1.3.4. PAMPA-BBB Assay

The blood-brain barrier (BBB) permeation is a prerequisite condition when screening CNS drugs. The BBB permeability of test compounds was screened through a parallel artificial membrane permeability assay (PAMPA) [197]. Porcine brain lipid (PBL) 4 µL dissolved in

dodecane (20mg/mL of PBL in dodecane) was coated on the bottom of the porous filter disks of receptor plates. The test compounds were prepared by dissolving compounds into DMSO and further diluted with PBS buffer (pH 7.4) to get a final concentration of 25 µg/mL. The donor plates (pore size 0.45 mm) were filled with 200 µL of test solution. The acceptor plate was placed on a donor plate-like sandwich and incubated for 18 h. Compounds absorbance was measured using a microplate reader (SpectraMax M5, US). The process was validated through eight commercial CNS drugs (progesterone, lomefloxacin, diazepam, alprazolam, oxazepam, atenolol, dopamine, and chlorpromazine) having known BBB permeability reports.

5.1.3.5. Evaluation of $A\beta_{1-42}$ aggregation inhibition activity

The $A\beta_{1-42}$ peptide was procured from Sigma-Aldrich, USA for assessment of $A\beta_{1-42}$ aggregation inhibition activity through thioflavin T assay [195,197,198]. The $A\beta_{1-42}$ (1 mg) was dissolved in 80 µL of 1 % NH_4OH and made up to 1mL with PBS 7.4 to get a stock solution of 1mg/mL. Further, working concentrations of $A\beta_{1-42}$ (10 µM) were prepared with PBS 7.4.

Self-induced $A\beta_{1-42}$ aggregation inhibition, $A\beta_{1-42}$ (10 µM: 2 µL) incubated with or without test compounds (5 µM, 10 µM, and 20 µM: 2 µL) at 37°C for 48 h. After incubation period, 20µM of 178 µL thioflavin T (ThT) was added to the previously incubated 96-well plates. The blank reading was taken using PBS buffer 7.4 instead of inhibitors. The fluorescence was measured at 450 nm (excitation) and 485 nm (emission) on microplate reader. The resulted data plotted graph as normalized fluorescence intensity (NFI) Vs with or without test compounds at different concentrations.

AChE induced $A\beta_{1-42}$ aggregation inhibition, the $A\beta_{1-42}$ (10 µM: 2 µL) and AChE (230 µM, 16 µL) from hAChE was incubated with or without test compounds (5 µM, 10 µM, and 20 µM: 2 µL) at 37°C for 48 h. After incubation period, 20 µM of 178 µL ThT was added to the

previously incubated 96-well plates. The blank reading was taken using PBS buffer 7.4 instead of inhibitors. The fluorescence was measured at 450 nm (excitation) and 485 nm (emission) on microplate reader. The resulted data plotted graph as normalized fluorescence intensity (NFI) Vs with or without test compounds at different concentrations.

Confocal fluorescence imaging, the $A\beta_{1-42}$ aggregation assay samples were further used for confocal imaging after 10-15 days of incubation period, samples were mounted on glass slides using 1,4-diazabicyclo [2.2.2] octane (DABCO) as a fixing agent. The images were captured at 20X (Carl Zeiss Microscopy GMBH, LSM 900) using fluorescence filter cubes at 494 nm and 518 nm respectively.

5.1.3.6. Evaluation of Neuroprotection activity

The neuroprotection activity of VA10 was evaluated against neuroblastoma cell line through an MTT assay [199]. The SH-SY5Y cells (density 1×10^5 cells/wells) were transferred into 96 well plates and incubated (24 h. at 37° C) in a humidified atmosphere with a 5 % CO_2 condition. Then, cells were treated with 10 µM of $A\beta_{1-42}$ for the next 24 h. The test compounds VA10 with different concentrations (5, 10, and 20 µM) were added, and cells were incubated for another 72 h. After, 20 µL of MTT reagent was added into wells and incubated for additional 2 h. Finally, observed purple-colored formazan crystals were solubilized into 100 µL of DMSO and absorbance was measured at 570 nm, and % cell viability results were calculated.

5.1.4. *In vivo* studies

5.1.4.1. Animals, housing, and materials

The male Wistar rats (200±15 g weight) were purchased from the Institute of Medical Science, Banaras Hindu University, Varanasi. These animals were housed in the environmentally controlled conditions of a 12 h day/night cycle, temperature (25±2°C), and humidity

(55±10RH) at Animal House, Department of Pharmaceutical Engineering and Technology, Indian Institute of Technology (BHU), Varanasi. Animals were allowed to acclimatize for 7 days. All the experimental protocols were approved (approval no. IIT(BHU)/IAEC/2022/022) by the Institutional Animal Ethical Committee, Indian Institute of Technology (BHU), Varanasi. All the chemicals (Scopolamine, $A\beta_{1-42}$, and, Donepezil, etc.) were purchased from commercial source Sigma-Aldrich, USA, and rat ACh ELISA kit was procured from Krishgen biosystems, India.

5.1.4.2. Acute oral toxicity evaluation

Evaluation of toxicity studies, OECD 423 guidelines were followed [200]. The acute toxicity studies were performed on female rats (n=6) by administering the VA10 orally. Rats were kept under observation for up to 24 h to identify behavioral changes, seizures, diarrhea, and mortality then, up to 14 days of normal observation [201]. After 14 days, animals were euthanized, and organs were isolated (brain, liver, kidney, and heart). The 10 μm thick transverse sections were taken using cryostat (SLEE MEV, Germany) and mounted on glass slides, and stained with hematoxylin and eosin. The slides were observed under a bright field microscope (Magnus MLX plus) at 10X resolution to identify possible damage to the organs.

5.1.4.3. Scopolamine induced amnesia (Y-maze test)

The Y maze test was conducted to assess spatial working memory in scopolamine-induced amnesic rats. The animal was divided into six groups and each group consists of six rats (n=6) i.e., group 1 normal control (vehicle alone, p.o.), group 2 disease control (scopolamine 0.5 mg/kg, i.p.), group 3 VA10 (2.5 mg/kg p.o.), group 4 VA10 (5 mg/kg p.o.), group 5 VAS (10 mg/kg p.o.), group 6 DPZ (5 mg/kg p.o.). Groups 1 and 2 received 0.5% carboxy methyl cellulose (vehicle alone) for up to 7 days. Whereas groups 3, 4, and 5 received VA10 2.5 mg/kg,

VA10 5 mg/kg, and VA10 10 mg/kg respectively, and group 6 received DPZ (5 mg/kg) as administered through an oral route (once a day for seven days). On seventh day (last day) of the experiment, the scopolamine (0.5 mg/kg, i.p.) was dissolved in normal saline and administered through i.p. rout to all groups of rats except group 1 (normal control). After, 30 min of scopolamine administration, spatial working memory was assessed through the Y-maze test. The animals were placed at the center of the arm and allowed to explore for 5 min. When the rat passes through all four paws into each arm considered arm entry. The percentage of spontaneous alterations was calculated by using the formula: [number of alterations/ (total arm entries-2) ×100] [202].

5.1.4.4. Morris water maze test

The $A\beta_{1-42}$ induced neurotoxic model was carried out to assess memory and learning impairment in rats through Morris water maze test [195,203]. Rats were randomly divided into four groups (n=6), normal control (sham), $A\beta_{1-42}$ control (negative control), VA10 (10 mg/kg p.o.), and DPZ (5 mg/kg p.o.). Animals were anesthetized using i.p. injection of ketamine and xylene mixture (dose of 90 and 9 mg/kg). Then, rats were placed on the stereotaxic apparatus, the head was fixed using ear bars and the scalp was incised and retracted. The head position was adjusted to locate the bregma and lambda region. The stereotaxic co-ordinates were set to bregma (-0.5 mm anteroposterior, +1.2 mm mediolateral, -3.2 dorsoventral and incision bar was set at -3.3 mm) [195]. Further, previously prepared $A\beta_{1-42}$ sterile saline injection (4 µM, 5µL) was infused into all groups except sham group through a Hamilton micro syringe at 2 µL/min. The syringe was kept for another 5min. to prevent efflux of infused solution. In sham group, saline was infused in place of $A\beta_{1-42}$.

After seven days of stereotaxic injection, treatment was started with test drug VA10 and DPZ for next seven days, and dose was administered through oral route once a day. Further,

assessment of memory and learning capacity was evaluated through behavioral studies, test apparatus (62 cm height, 32 cm depth, and 121 cm diameter) was equally divided into four quadrants filled with water (25±2°C), and titanium dioxide was used to make water opaque. In training trails, animal was placed into one quadrant facing toward the wall and allowed to find the hidden platform for 120 sec. The experiment was conducted for five days with four training trials per day (intra-trail interval is about 10 min). On sixth day (before probe trial), platform was removed and animals were allowed to swim for 120 sec to assess their spatial memory (Figure 5.2). The observed values (escape latency in training trails, time spent on platform, and number of entries to the platform zone) data were analyzed using GraphPad prism 5.

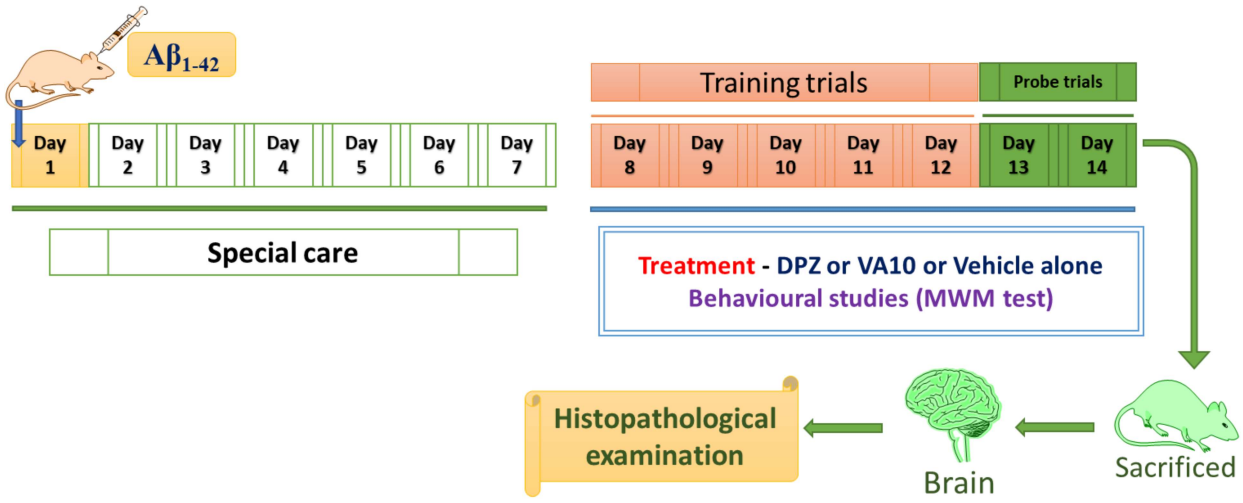

Figure 5.2. Schematic representation of $A\beta_{1-42}$ induced neurotoxic model

5.1.4.5. Ex-vivo neurochemical estimation

After completion of behavioral studies, all animals were euthanized and whole brain was isolated. The brain samples were homogenized with 10 mM PBS buffer (pH 7.4) and centrifuged (4°C) at 4350 g for 15 min. The obtained supernatants were separated and tested for AChE activity using previously reported Ellman method [204] and Acetylcholine (ACh) was estimated using a rat acetylcholine ELISA (Krishgen Biosystems, India) kit. Estimation of

AChE, 100 µL of supernatant was incubated with 15 mM of 100 µL ATCI (prepared in PBS buffer 7.4) for 5min. followed by addition of 100 µL of 1.5 mM DTNB and absorbance was measured at 415 nm. The rate of hydrolysis was calculated as µM of substrate hydrolyzed/min/mg of protein. The enzyme immunoassay for the quantitative determination of rat acetylcholine (ACh) in the brain was performed as per the protocol given in ELISA kit.

5.1.4.6. Nissl Staining

After completion of Morris water maze test, animals were euthanized, and whole brain was isolated for evaluating neuronal cell density at hippocampus region [205]. The whole brains were washed with saline, transferred into a 4 % paraformaldehyde solution, and kept at 4°C overnight. Then, transferred into 15 % of sucrose solution (in PBS) and 30 % sucrose (in PBS). Further, embedding was done in an optimum cutting temperature (OCT) solution, 10µm thick transverse sections were cut by a cryostat (SLEE MEV, Germany) and mounted on poly-L-lysine coated slides. These sections were hydrated in 95 % ethyl alcohol solution at room temperature for 5 h, rinsed in 75 % of ethyl alcohol for 5 min, and then distilled water for another 5 min. After, incubation in 1 % cresyl violet acetate (warmed at 50-60°C) for 20 min., rinsed in water for 5 min and dehydrated at 75 % alcohol for a few seconds, 95 % ethyl alcohol for 2 min, and then absolute alcohol for 2 min. Finally, they were cleared in xylene for 2-3 min and mounted with DPX. The slides were observed under a bright field microscope (Magnus MLX plus, India) at 4X and 10X resolution, and cell density was calculated using ImageJ software (NIH, USA).

5.1.5. Statistical analysis

The statistical data were expressed in mean ± standard deviation (S.D). Graph pad prism 5 software was used to analyze the data. All the results were analyzed by one-way ANOVA followed by Tukey's post hoc test, except escape latency in MWM, which was analyzed by

two-way ANOVA followed by Bonferroni's post hoc test. A P-value of less than 0.05 was considered statistically significant.

5.2. Results and discussion

5.2.1. Extraction and isolation of vasicine

The methanolic extract of *Adhatoda vasica* leaves was prepared by maceration technique and extractive value was found to be 12.6 g/kg w/w. Further, vasicine (VAS) was isolated from methanolic extract through column chromatography, in fraction number 100-125 compound VAS was identified with a yield of 0.43 g/kg w/w of dried leaves.

5.2.2. Design and synthesis of vasicine derivatives

Synthesis of 3-OH pyrrolidine derivatives, reaction was started by cleavage of imidine bond of vasicine (VAS) [10] using $NaBH_4$ in water/MeOH (1:1) to get key intermediate compound 1-(2-amino benzyl) pyrrolidine-3-ol (VA) [206]. Further, coupling of compound VA with various substituted carboxylic acids (1-25) to achieve final compounds (VA01-VA25) (Scheme 5.1) [195]. These synthesized compounds were purified through column chromatography by following chromatographic conditions i.e., silica gel (60-120 mesh) was used as a stationary phase, and mobile phase was optimized as ethyl acetate (70): hexane (30). The resulted compounds were characterized by ^{1}H NMR, ^{13}C NMR, and HRMS techniques. In addition, compounds containing amide -NH and hydroxyl group -OH were established by ^{1}H NMR through D_2O exchange analysis. Furthermore, structural confirmation of hit compound VA10 (4-Bromo substituted) was characterized by SC-XRD analysis. The compound L-VA10 formed large crystals upon dissolved in hot ethanol and filtered, then slow evaporation, allowing the structural determination through SC-XRD (Figure 5.3, Scheme 5.1).

Scheme 5.1. Synthesis of vasicine hybrids VA01 to VA25[a]

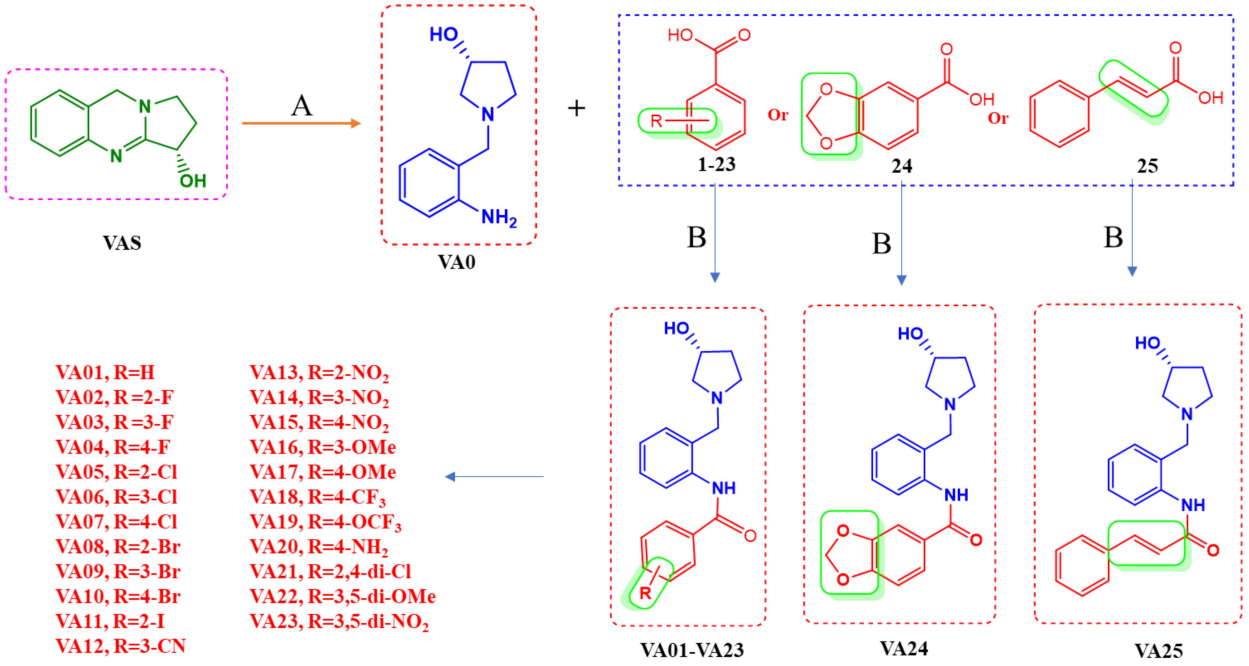

[a] Reagents and conditions: (A) Vasicine (VA) 1.0 *eq*, $NaBH_4$ 3.0 *eq*, H_2O/MeOH (1:1), r.t., 4h. (B) 1-(2-amino benzyl) pyrrolidine-3-ol (VA0) 1.0 *eq*, carboxylic acids (1-25) 1.2 *eq*, Diisopropylethylamine (DIPEA) 2.5 *eq*, 1-Hydroxybenzotriazole (HOBT) 2.5 *eq*, 1-(3-Dimethylaminopropyl)-3-ethyl carbodiimide hydrochloride (EDC.HCL) 1.5 *eq*, Acetonitrile, r.t., 8h.

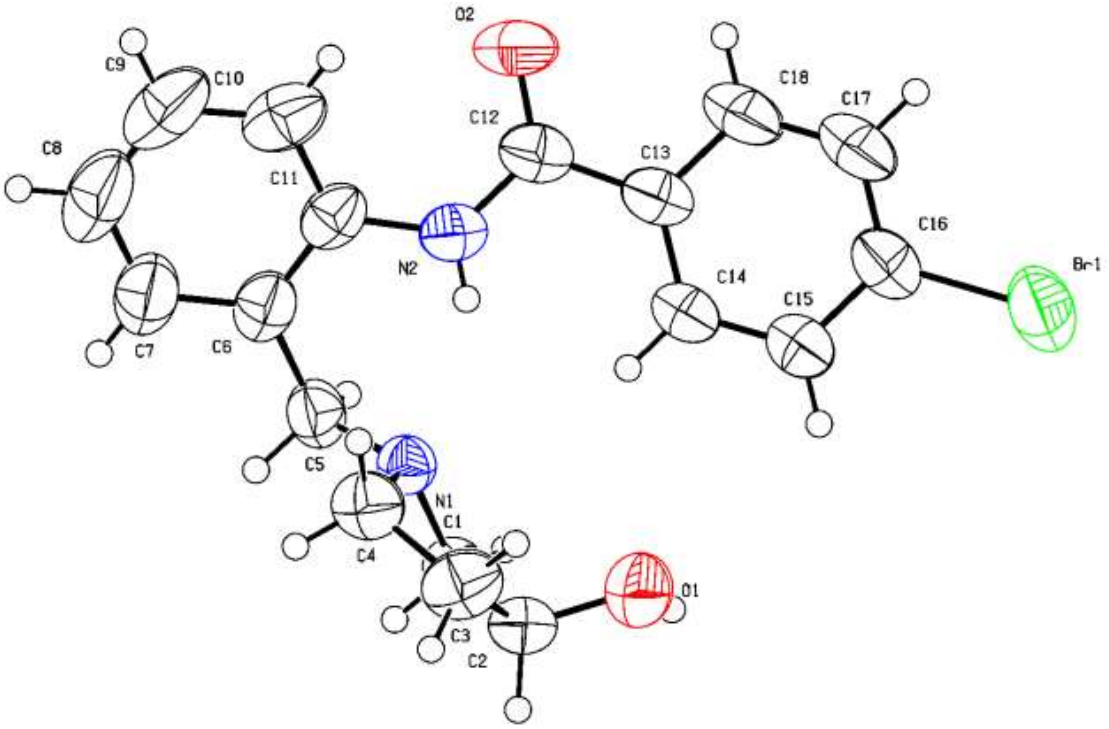

Figure 5.3. ORTEP diagram of compound L-VA10 (40 % ellipsoid plot)

Table 5.1. Crystal data and structure refinement for compound VA10

Structural parameters	**Compound VA10**	**Structural parameters**	**Compound VA10**
Empirical formula	$C_{18}H_{19}BrN_2O_2$	**Reflections collected / unique**	34455 / 3326 [R(int) = 0.0466]
Formula weight	375.26	**Completeness to theta = 67.679**	99.9 %
Temperature	298(2) K	**Absorption correction**	Semi-empirical from equivalents
Wavelength	1.54178 A°	**Max. and min. transmission**	0.7533 and 0.6500
Crystal system, space group	Orthorhombic, P 21 21 21	**Refinement method**	Full-matrix least-squares on F^2
Unit cell dimensions	a = 9.8116(2) A, alpha = 90 $^{\circ}$. b = 11.3435(2) A, beta = 90 $^{\circ}$. c = 15.8060(3) A, gamma = 90 $^{\circ}$.	**Data/restraints/parameters**	3326 / 36 / 201
Volume	1759.17(6) A^3	**Goodness-of-fit on F^2**	0.875

Z, Calculated density	4, 1.417 Mg/m^3	**Final R indices [I>2sigma(I)]**	R_1 = 0.0384, wR_2 = 0.1019
Absorption coefficient	3.271 mm^{-1}	**R indices (all data)**	R_1 = 0.0438, wR_2 = 0.1099
F(000)	768	**Absolute structure parameter**	0.018(8)
Crystal size	0.158 x 0.118 x 0.115 mm	**Extinction coefficient**	0.0052(5)
Theta range for data collection	4.798 to 70.028°.	**Largest diff. peak and hole**	0.320 and -0.394 $e.A^{-3}$
Limiting indices	11<=h<=11, -13<=k<=13, -19<=l<=19	-	-

5.2.3. *In silico* studies

5.2.3.1. Molecular docking studies on AChE

The docking studies were performed on all synthesized compounds within the active site of recombinant human AChE enzyme (Table 5.2). The compounds showed binding energies between -8.86 to -10.37 kcal/mol and formed interactions with surrounding amino acid residues at active sites, Such as Trp86, Ser293, Phe295, Arg296, Phe338, Tyr341, Leu286, Trp286, Tyr337, Phe338, and Tyr341. The docking parameters were validated by superimposition of donepezil (DPZ) over docked conformers of compounds at active site of AChE. The hit compound VA10 formed interactions with Ser293 (H bond), Phe295 (H bond), Arg296 (H bond), Phe338 (π-π stacked), Tyr341 (π-π t-shaped), Leu286 (alkyl), Trp286 (π-alkyl), Tyr337 (π-alkyl), Phe338 (π-alkyl), and Tyr341 (π-alkyl) at AChE active site (Figure 5.4). These ligand-protein binding interaction figures of compound VA10 and reference DPZ were depicted (2D and 3D) in Figure 5.4.

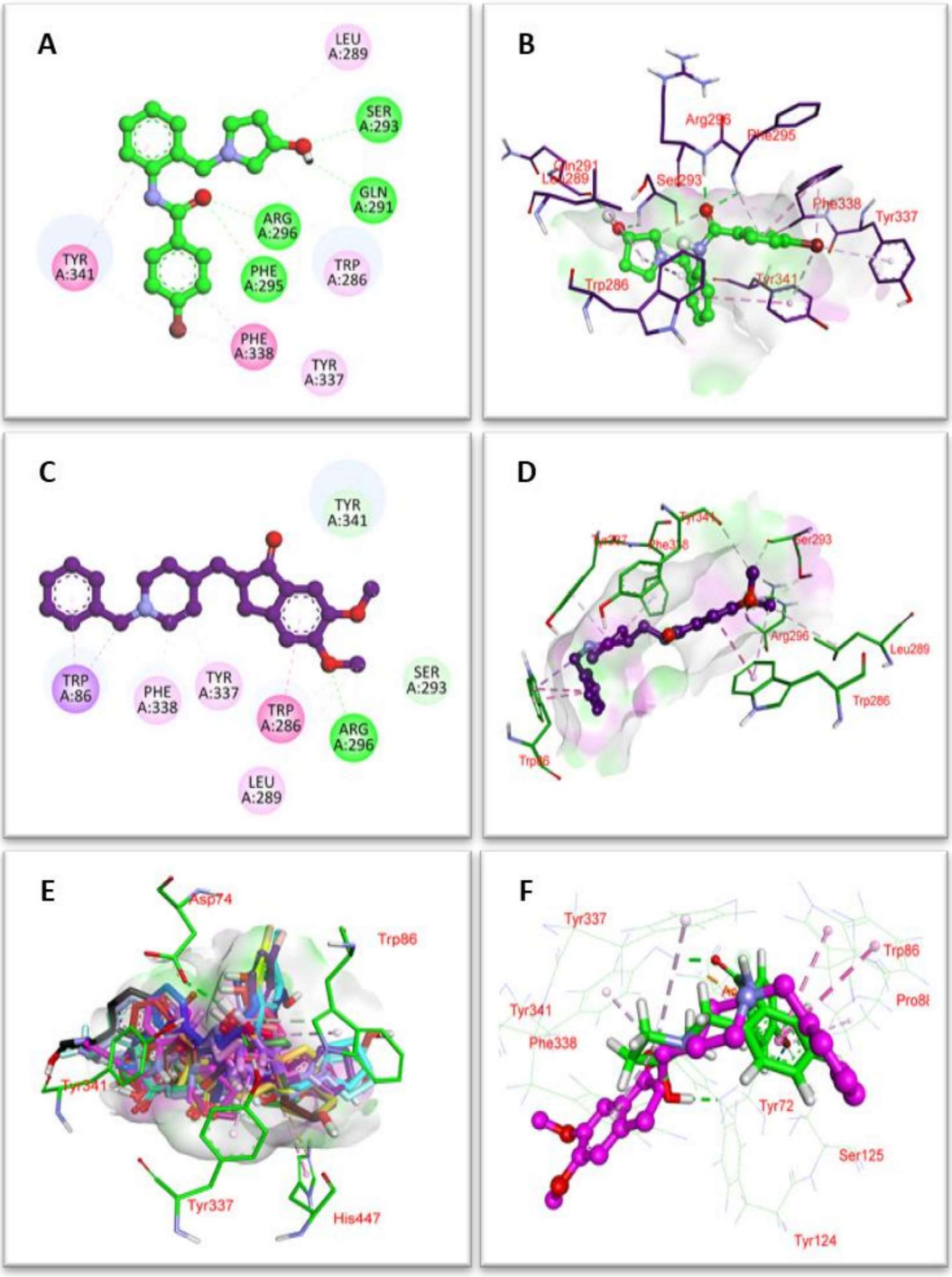

Figure 5.4. The binding interactions of VA10 and DPZ at AChE active site. (A, B) depicts the interaction of VA10 with AChE, (C, D) depicts the interaction of DPZ with AChE, (E) depicts all docked ligands at AChE site, and (F) depicts superimposition of compound VA10 (green) over DPZ (purple) at AChE site.

5.2.3.2. Molecular docking studies on BuChE

The synthetic compounds were docked at human BuChE active site and results were validated by comparing them with reference inhibitor tacrine (Table 5.2). The docked compounds showed binding energies between -7.51 Kcal/mol to -8.51 Kcal/mol. The hit compound VA10 formed interactions with Gly78 (H-bond), Trp82 (π-π stacked, π-alkyl), Trp231 (π-alkyl), Ala328 (Alkyl), Phe329 (π-π t-shaped), Phe398 (π-alkyl), His438 (H-bond), Tyr440 (H-bond). These ligand-protein binding interaction figures of compound VA10 and reference tacrine were depicted (2D and 3D) in Figure 5.5.

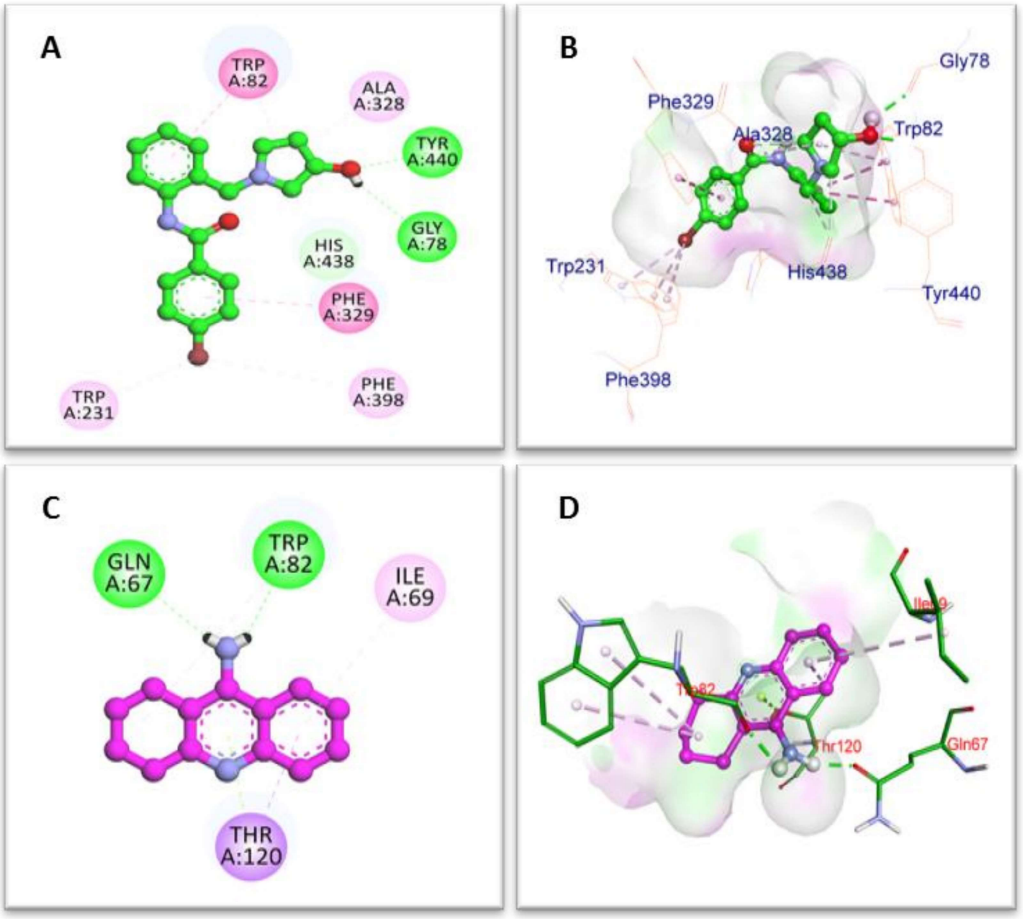

Figure 5.5. The binding interactions of VA10 and tacrine at BuChE active site. (A, B) depicts the interaction of VA10 with BuChE, and (C, D) depicts the interaction of tacrine with BuChE.

Table 5.2. Molecular docking studies on vasicine derivatives

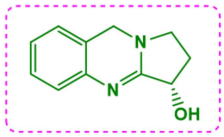

VAS

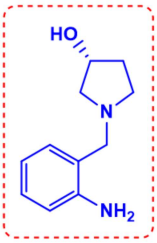

VA

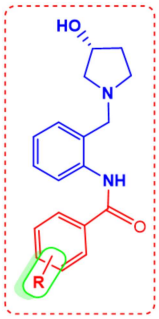

VA01-VA23

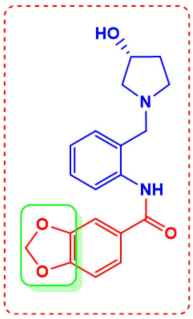

VA24

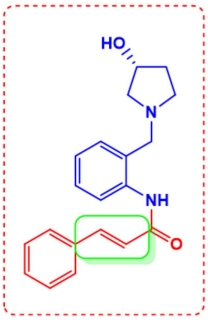

VA25

S.no.	Compound	R	AChE binding energy (Kcal/mol)	Ligand efficiency	BuChE binding energy (Kcal/mol)	Ligand efficiency
1	VAS	-	-6.79	-0.49	-5.93	-0.42
2	VA	-	-6.82	-0.49	-5.61	-0.40
3	VA01	H	-8.86	-0.40	-7.85	-0.36
4	VA02	2-F	-8.84	-0.39	-7.74	-0.34
5	VA03	3-F	-8.89	-0.39	-7.68	-0.33
6	VA04	4-F	-9.00	-0.39	-7.69	-0.33
7	VA05	2-Cl	-9.76	-0.42	-8.19	-0.36
8	VA06	3- Cl	-10.03	-0.44	-8.40	-0.37
9	VA07	4-Cl	-9.60	-0.48	-8.44	-0.37
10	VA08	2-Br	-10.37	-0.45	-8.39	-0.36
11	VA09	3-Br	-10.01	-0.44	-8.51	-0.37
12	VA10	4-Br	-10.02	-0.46	-8.42	-0.37
13	VA11	2-I	-9.17	-0.32	-8.12	-0.36
14	VA12	3-CN	-9.81	-0.39	-8.23	-0.34
15	VA13	2-NO_2	-9.87	-0.41	-7.66	-0.32

16	VA14	3-NO_2	-10.01	-0.40	-7.51	-0.30
17	VA15	4-NO_2	-9.73	-0.39	-7.64	-0.31
18	VA16	3-OMe	-9.99	-0.42	-7.94	-0.33
19	VA17	4-OMe	-9.44	-0.39	-7.74	-0.32
20	VA18	4-CF_3	-10.02	-0.39	-7.69	-0.30
21	VA19	4-OCF_3	-9.89	-0.38	-7.62	-0.29
22	VA20	4-NH_2	-9.73	-0.32	-8.16	-0.27
23	VA21	2,4-di-Cl	-10.30	-0.39	-8.06	-0.30
24	VA22	3,5-di-OMe	-9.06	-0.40	-7.68	-0.31
25	VA23	3,5-di-NO_2	-10.09	-0.41	-7.82	-0.29
26	VA24	-	-10.52	-0.42	-8.27	-0.33
27	VA25	-	-10.21	-0.41	-8.51	-0.33
28	Donepezil	-	-11.8	-0.42	-	-
29	Tacrine	-	-	-	-6.75	-0.45

5.2.3.3. Molecular dynamic simulation studies on AChE

The interaction stability profile and mode of interactions between compound VA10 and AChE were analyzed through molecular dynamics (MD) simulations studies (Figure 5.6). The MD simulations were performed for 100 ns, and the overall stability of the simulation was evaluated using the root mean square deviations (RMSD) of the backbone atoms, which ranged from 0.2 to 1.7 A°. The graph suggests that the RMSD of the protein backbone is stable throughout the MD simulation and attains equilibrium within 5 ns. The ligand root means square fluctuation (L-RMSF) profile indicated ligand fragments interact with the protein and play an entropic role in the binding event. The stacked bar diagram indicates normal interactions throughout the MD

simulations. The bar chart showed three types of ligand-protein interactions, which includes H-bonding, hydrophobic interactions, and water bridge.

Hydrogen bond interactions formed between compound VA10 and AChE residues are Asp74, Gly121, Tyr124, Ser125, Trp286, Glu292, Ser293, Phe295, Arg296, Tyr337, and Tyr347. The hydrogen bond can influence drug specificity, adsorption, and metabolism. It was also observed that compound VA10 formed hydrophobic interactions viz., Tyr72, Val73, Phe80, Trp86, Tyr124, Trp286, Val294, Phe297, Tyr337, Phe338, and Tyr341. There is no ionic bond interaction was observed. The water bridges are formed by a water molecule, which were formed hydrogen bond between protein and ligand. Further, observed water bridges are Val73, Asp74, Tyr77, Pro78, Gly82, Tyr124, Trp286, Glu292, Ser293, Phe295, Arg296, Ser298, Tyr337, Tyr341 and Lys348. The ligand RMSF, Protein RMSF, protein RMSD, ligand RMSD, and interaction fractions results were analyzed and graphs were shown in Figure 5.6.

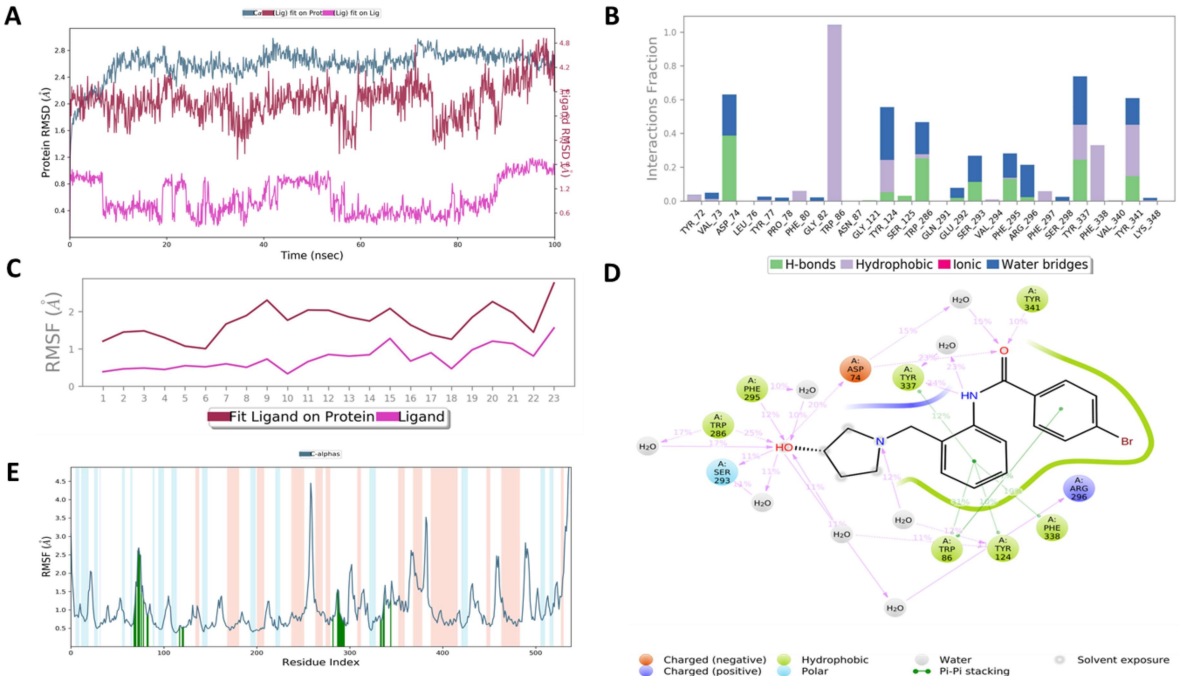

Figure 5.6. VA10 modulates the AChE interactions on molecular dynamic simulations, (A) depicts the protein root mean square deviation (RMSD) (left Y-axis) and ligand RMSD (right Y-axis) indicating the stability of ligand VA10 with respect to protein AChE, (B) showing bar

charts of ligand-protein interactions throughout the simulation (Green- H-bonding; light purple- hydrophobic; Blue-water bridges), (C) depicts the ligand VAS Root mean square fluctuation (RMSF) and stability at active site, (D) depicts ligand contacts with AChE residues, and (E) showing the RMSF plot of protein AChE during simulation.

5.2.4. Analysis of Drug-likeness, ADME, and toxicity parameters

Synthesized compounds (VA01-VA25) including precursor vasicine and key intermediate screened through swissADME and preADMET tools. All the tested compounds were obeying drug-likeness parameters according to Lipinski's rule of five. Further, ADME prediction of compounds revealed that compounds have membrane permeation ability for human intestinal absorption (HIA). Moreover, Madin-Darby canine kidney permeability (MDCK) and Caco2 cell permeation results that ligands can be absorbed through oral route. Skin permeation data suggested that compounds have low skin permeability. In addition, toxicity prediction results suggested that compounds have no toxic effects in mice and rats. The cardiotoxicity (hERG) prediction indicates that low risk against hERG channel. The obtained results of most active compound VA10 were presented in Table 5.3.

Table 5.3. Drug-likeness, ADME, and Toxicity prediction of compound VA10

S. No	Parameters	Compound VA10
Physicochemical Properties/Drug likeness		
1	Formula	$C_{18}H_{19}BrN_2O_2$
2	Molecular weight	326.39
4	No. rotatable bonds	6
5	No. H-bond acceptors	4
6	No. H-bond donors	2
7	TPSA	61.80
8	Log Po/w	2.22
ADME		
9	BBB	1.33406
10	Buffer solubility (mg/L)	269.127
11	*In vitro* Caco-2 cell permeability (nm/sec)	23.77
13	CYP_2D6_inhibition	Inhibitor
14	CYP_3A4_inhibition	Weakly
15	CYP_3A4_substrate	Inhibitor
16	Human intestinal absorption (HIA %)	93.63

17	*In vitro* MDCK cell permeability (nm/sec)	18.03
18	*In vitro* P-glycoprotein inhibition	non
19	*In vitro* plasma protein binding (%)	49.54
20	*In vitro* skin permeability (log Kp, cm/hour)	3.57
Toxicity		
21	Acute algae toxicity	0.0280
22	Ames test	Mutagen
23	Carcinogenicity (Mouse)	Negative
24	Carcinogenicity (Rat)	Negative
25	Acute daphina toxicity	0.0704
26	*In vitro* hERG inhibition	Medium risk
27	Acute fish toxicity (medaka)	0.00988
28	Acute fish toxicity (minnow)	0.0291

5.2.5. *In vitro* studies

5.2.5.1. Cholinesterase inhibition and SAR studies

The deficiency of acetylcholine is one of the major factors to develop Alzheimer's disease. Previous clinical reports suggested that cholinesterase inhibitors are effective to acts on improving behavior and decreasing cognitive decline [207]. The hit compound VA10 (hAChE IC_{50}: 0.25±0.003 μM; eeAChE IC_{50}: 0.23±0.005 μM; eqBuChE IC_{50}: 0.72±0.012 μM) showed most significant inhibitory profile to DPZ among all tested analogs (Table 5.4).

The cholinesterase inhibition data suggested that bromo substitution at para position may possess most selective cholinesterase inhibition (Table 5.4) and also, Para substituted derivatives showed high potency compared to ortho and meta substituents. The compounds which contain electron-donating groups displayed more cholinesterase inhibition when compared to electron-withdrawing groups. Further, compounds with nitro substitution at ortho, meta, and para positions showed less inhibitory activity suggesting that nitro compounds decreased the compound potency. The compound (VA24) showed moderate activity and low selectivity towards cholinesterase inhibition by increasing bulkiness of compound, indicating that no need to increase compound bulkiness. Compound (VA25) with increasing number of

carbons chain between carbonyl carbon and substituted aromatic ring, observed that there is no improvement in potency.

Table 5.4. Structures, Cholinesterase (AChE and BuChE) inhibitory activity, and PAMPA assay of vasicine derivatives

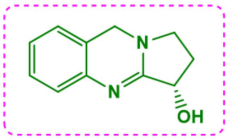

VAS

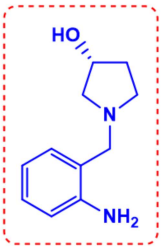

VA

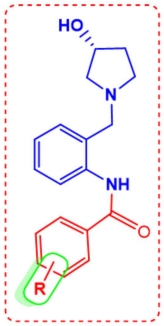

VA01-VA23

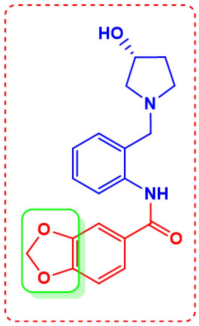

VA24

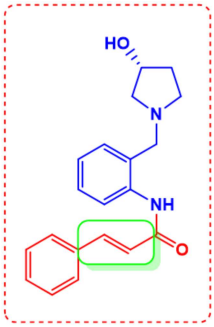

VA25

S. No.	Comp.	R	eeAChE IC_{50} (µM) [a]	hAChE IC_{50} (µM) [a]	eqBuChE IC_{50} (µM) [a]	Pe (10^{-6} cm s^{-1}) [a, b]	CNS (+/-)
1	VAS	-	3.13±0.11	2.96±0.09	5.61±0.133	4.8±0.0515	CNS^+
2	VA	-	3.06±0.081	nd	5.23±0.094	4.94±0.0431	CNS^+
3	VA01	H	1.90±0.027	1.86±0.024	3.92±0.051	9.12±0.135	CNS^+
4	VA02	2-F	1.13±0.019	nd	3.11±0.037	10.15±0.163	CNS^+
5	VA03	3-F	1.26±0.032	nd	3.18±0.032	10.19±0.147	CNS^+
6	VA04	4-F	0.94±0.016	1.03±0.015	1.92±0.025	10.21±0.174	CNS^+
7	VA05	2-Cl	1.34±0.022	nd	3.28±0.039	9.81±0.153	CNS^+
8	VA06	3- Cl	1.09±0.018	nd	2.76±0.034	9.93±0.144	CNS^+
9	VA07	4-Cl	0.55±0.011	0.59±0.013	1.83±0.030	10.04±0.192	CNS^+
10	VA08	2-Br	1.29±0.024	nd	2.67±0.046	10.15±0.133	CNS^+
11	VA09	3-Br	0.98±0.014	nd	1.51±0.027	10.21±0.139	CNS^+
12	VA10	4-Br	0.23±0.005	0.25±0.003	0.72±0.012	10.56±0.154	CNS^+
13	VA11	2-I	1.32±0.017	nd	3.19±0.038	9.83±0.132	CNS^+
14	VA12	3-CN	0.96±0.013	nd	1.98±0.026	8.67±0.122	CNS^+

15	VA13	2-NO_2	3.17±0.065	nd	4.13±0.053	7.56±0.137	CNS^+
16	VA14	3-NO_2	2.98±0.053	nd	3.74±0.047	7.71±0.144	CNS^+
17	VA15	4-NO_2	1.27±0.027	nd	2.72±0.052	7.93±0.126	CNS^+
18	VA16	3-OMe	1.79±0.032	nd	2.09±0.041	9.82±0.141	CNS^+
19	VA17	4-OMe	1.09±0.018	1.01±0.016	1.87±0.022	10.12±0.163	CNS^+
20	VA18	4-CF_3	1.54±0.023	nd	2.36±0.030	10.16±0.157	CNS^+
21	VA19	4-OCF_3	1.28±0.019	nd	2.92±0.029	10.43±0.162	CNS^+
22	VA20	4-NH_2	1.16±0.017	nd	2.43±0.037	9.54±0.143	CNS^+
23	VA21	2,4-di-Cl	1.07±0.014	nd	1.95±0.026	10.42±0.139	CNS^+
24	VA22	3,5-di-OMe	1.95±0.021	nd	2.89±0.032	9.98±0.134	CNS^+
25	VA23	3,5-di-NO_2	3.95±0.074	nd	4.19±0.054	7.79±0.128	CNS^+
26	VA24	-	2.15±0.036	2.03±0.031	4.64±0.051	10.52±0.159	CNS^+
27	VA25	-	2.06.1±0.043	2.09±0.039	4.50±0.047	9.84±0.133	CNS^+
28	DPZ	-	0.041±0.0008	0.036±0.0007	1.09±0.016	7.96±0.146	CNS^+

[a] data expressed in three independent experiments (mean±SD, n=3); [b] compound with pe > 4.32×10^{-6} cm s^{-1} could cross BBB (CNS^+). Compound with pe < 1.84×10^{-6} cm s^{-1} does not cross the BBB (CNS^-). Compounds with pe > 1.84×10^{-6} cm s^{-1} to pe < 4.32×10^{-6} cm s^{-1} uncertain BBB permeation (CNS±). nd: not determined.

5.2.5.2. Free-radical scavenging assay

In AD conditions, oxidative stress may increase disease complexity by producing reactive oxygen species [194]. It may leads to impairment in cellular functions and can be one of the reasons for neurodegeneration. The tested compound VA10 showed significant antioxidant activity among all tested analogs and results were significant to reference compound ascorbic acid (AA) ($P<0.0001$). The compounds are probably exerting their antioxidant activity through free radical scavenging potency by transferring hydrogen atoms to their substrates. The

obtained DPPH assay results were expressed in the form of IC_{50} (μM) value, it defined as the concentration of antioxidant species required for reduction of 50 % of the DPPH radical concentration in a solution (Table 5.5).

Table 5.5. Antioxidant activity (DPPH assay) of compounds VA04, VA07, VA10, and VA17

Compound	DPPH assay IC_{50} (μM)[a]
VA04	30.30±0.97
VA07	27.71±0.91
VA10	24.12±0.79
VA17	33.32±0.82
VAS	37.29±0.85
AA	26.71±0.89

[a] Data expressed as the mean±SD of three independent experiments. AA: Ascorbic acid

5.2.5.3. Propidium iodide displacement assay

In general, specific ligands, which may bind to AChE peripheral anionic site (PAS) property was evaluated through propidium iodide assay [208]. The hit compound VA10 affinity towards the PAS of AChE was estimated with different concentrations (5, 10, 20 μM) (Table 5.6). Propidium iodide fluorescence was decreased in the presence of compound VA10 in a concentration-dependent manner, which indicates that test compound interrupted specific PAS site by propidium displacement. Reference drug DPZ, which is known to bind at PAS site used as positive control. The resulted data indicate that there is no significant difference between DPZ (20 μM) and VA10 (20 μM) ($P<0.0001$).

Table 5.6. Propidium iodide displacement assay

Compound	Displacement of propidium iodide from AChE PAS (% inhibition) [a]		
	Concentration (5 µM)	Concentration (10 µM)	Concentration (20 µM)
VA10	17.50±0.40	31.16±0.62	51.73±0.81
DPZ	-	-	52.11±0.67

[a] Data expressed as the mean±SD of three independent experiments.

5.2.5.4. BBB-PAMPA assay

Permeation through the blood-brain barrier (BBB) is a necessary factor for CNS targeting drugs [209]. The synthesized compounds BBB permeability was estimated through parallel artificial membrane permeation assay (PAMPA) to confirm their lipophilicity. The tested compounds are permeable as per in-vitro predictions and compounds showed significant permeability profiles, which suggested that compounds may cross BBB (Table 5.4).

5.2.5.5. Self-induced and hAChE induced $A\beta_{1-42}$ aggregation (thioflavin T assay)

Cholinesterase inhibitors bind to PAS region and prevents Aβ production and deposition, the inhibitory potency of compound VA10 was evaluated using thioflavin T (ThT) [198] by self-induced $A\beta_{1-42}$ aggregation and hAChE-induced $A\beta_{1-42}$ aggregation assay (Figure 5.7). The hit compound VA10 exhibited moderate anti-aggregatory potency at a concentration of 5µM and 10 µM. Further, compound VA10 at a higher concentration (20 µM) exhibited significant inhibition as compared to positive control DPZ (20 µM) ($P<0.0001$) on both experiments self-induced and $A\beta_{1-42}$ aggregation assays. In addition, confocal microscopic (20X magnification) analysis was also carried out to observe the $A\beta_{1-42}$ aggregates size of compound VA10 treated and nontreated samples. The results suggested that absence of inhibitor (consisting of $A\beta_{1-42}$ with ThT only) showed large-size aggregates and samples treated with VA10 showed very smaller size aggregates in a concentration-dependent manner. These experimental data indicate

that compound VA10 can able to inhibits self-induced $A\beta_{1-42}$ aggregation as well as hAChE-induced $A\beta_{1-42}$ aggregation when compared to DPZ (Figure 5.7).

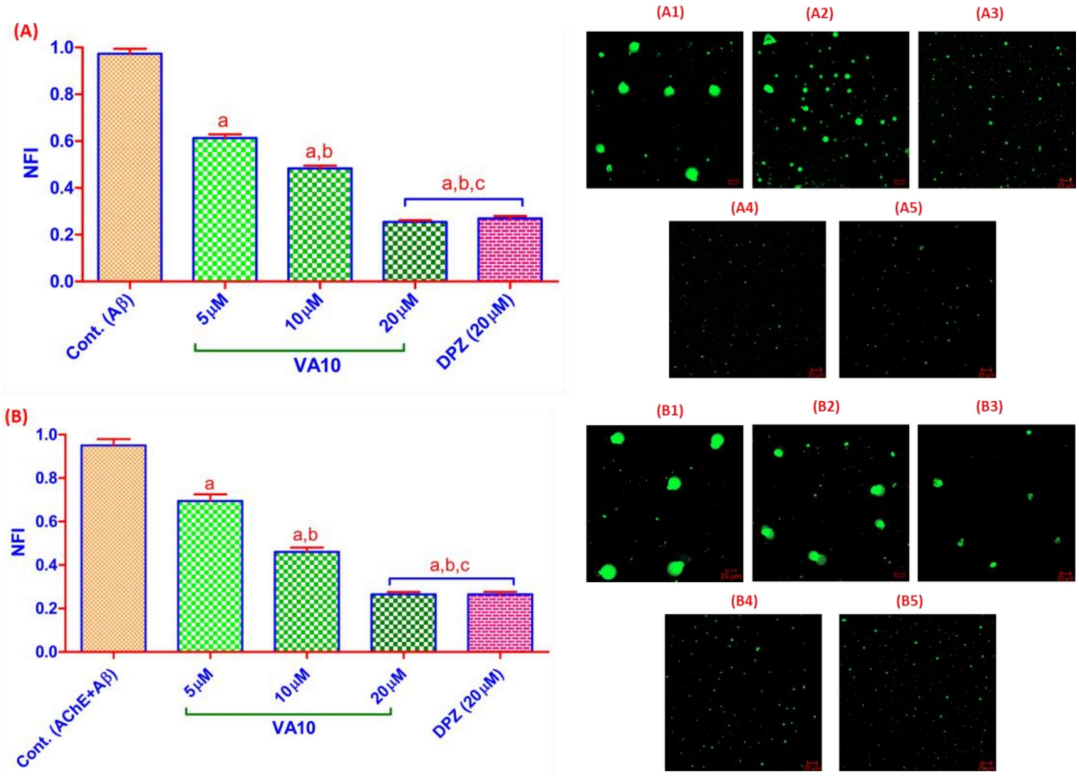

Figure 5.7. Effect of compound VA10 on $A\beta_{1-42}$ aggregation inhibition. (A) showing inhibitory potency of compound VA10 on $A\beta_{1-42}$ aggregation, (A1) showing effect of $A\beta_{1-42}$ aggregates without inhibitor, (A2) showing effect of VA10 (5μM) on $A\beta_{1-42}$ aggregates, (A3) showing effect of VA10 (10μM) on $A\beta_{1-42}$ aggregates, (A4) showing effect of VA10 (20μM) on $A\beta_{1-42}$ aggregates, and (A5) showing effect of DPZ (20μM) on $A\beta_{1-42}$ aggregates. (B) showing inhibitory potency of compound VA10 on AChE induced $A\beta_{1-42}$ aggregation. (B1) shows effect of hAChE induced $A\beta_{1-42}$ aggregates without inhibitor, (A2) shows effect of VA10 (5μM) on hAChE induced $A\beta_{1-42}$ aggregates, (A3) shows effect of VA10 (10μM) on hAChE induced $A\beta_{1-42}$ aggregates, (A4) showing effect of VA10 (20μM) on hAChE induced $A\beta_{1-42}$ aggregates, and (A5) showing effect of DPZ (20μM) on hAChE induced $A\beta_{1-42}$ aggregates. $^{a}P<0.05$ compared to control, $^{b}P<0.05$ compared VA10 (5μM), $^{c}P<0.05$ compared VA10 (10μM). (Mean ± SD, n=3. One-way ANOVA followed by Tukey's post hoc test). NFI: nominal fluorescence intensity.

5.2.5.6. Neuroprotection activity

The cell line studies are helpful for the primary optimization and mechanistic investigations on test compounds for further animal-based toxicological studies [210]. Estimation of neuroprotection potency and toxicity of compound VA10 was evaluated through MTT assay by using human neuroblastoma cell line (SH-SY5Y). $A\beta_{1-42}$ peptide is the most amyloidogenic and neurotoxic isoform of $A\beta_{1-42}$ and was used at a concentration of 10 µM to promote toxicity on cell lines. The experimental data revealed that compound VA10 reduced the $A\beta_{1-42}$ aggregation and showed no toxic effects on tested cell line (SH-SY5Y). These results (Figure 5.8) suggests that treatment of SH-SY5Y cells with $A\beta_{1-42}$ peptide significantly decreased the cell viability. The hit compound VA10 demonstrated that there is no significant difference in cytotoxicity profile as compared to DPZ at a concentration of 20 µM ($P<0.0001$).

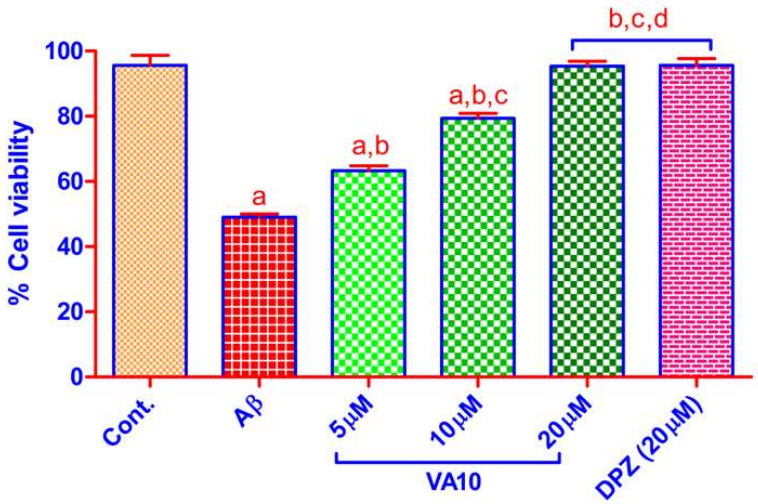

Figure 5.8. Depicts the effect of VA10 on SH-SY5Y cells. [a]$P<0.05$ compared to control, [b]$P<0.05$ compared to $A\beta_{1-42}$, [c]$P<0.05$ compared to $A\beta_{1-42}$ with VA10 (5µM), [d]$P<0.05$ compared to $A\beta_{1-42}$ with VA10 (10µM). One-way ANOVA followed by Tukey's post hoc test (n=3).

5.2.6. *In vivo* studies

5.2.6.1. Acute oral toxicity studies

The acute toxicity of compound VA10 was determined on healthy Wistar female rats as per OECD guidelines. From the dose of administration to day 14, there is no notable toxicity symptoms were observed i.e., death, abnormal behavior, changes in water or food consumption, mortality, and weight loss (Table 5.7). Further, various biochemical indices like alanine transaminase (ALT), aspartate transaminase (AST), alkaline phosphatase (ALP), creatinine, and creatine kinase- myocardial band (Ck-MD) confirmed that VA10 did not cause organ toxicity (Table 5.8) up to 300 mg/kg. In addition, histological observations were carried out on brain, liver, heart, and kidney, which suggests that test compound VA10 showed no notable toxicity/damage in observed organ tissues as compared to control group (Figure 5.9). The sections were reported in 10X resolution under bright field microscope.

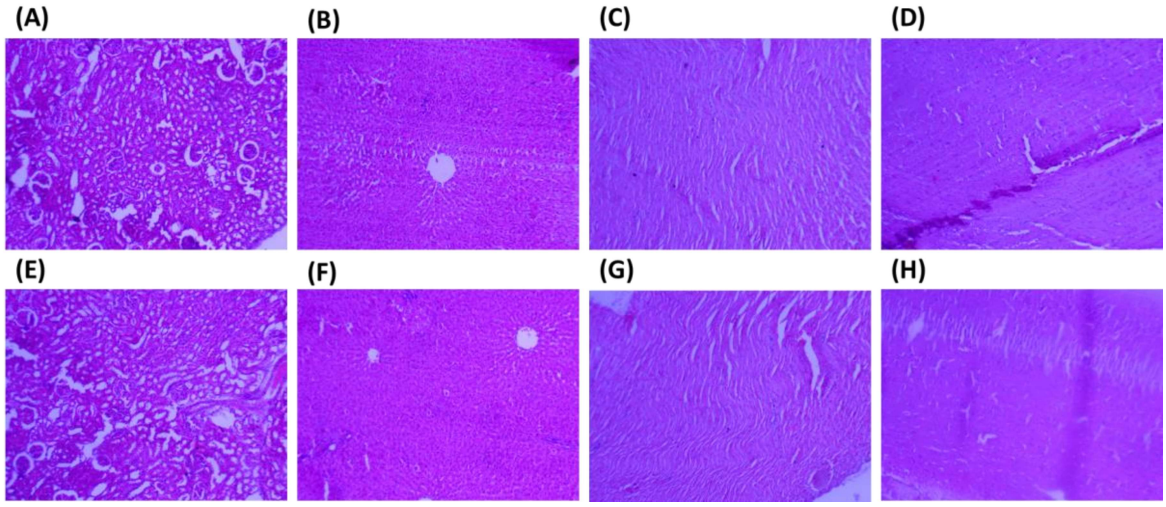

Figure 5.9. Effect of VA10 treatment on organ toxicity. (A), (B), (C), and (D) indicates the effect of control group (vehicle alone) on kidney, liver, heart, and brain, respectively. (E), (F), (G), and (H) indicates the effect of VA10 treatment on kidney, liver, heart, and brain, respectively.

Table 5.7. Effect of single dose oral administration of VA10 on body weight of rats

No. of days	Normal control [a] (Body weight in grams)	Compound VA10 (300 mg/kg) [a] (Body weight in grams)
0th day	200.67±10.47	203.09±11.82
7th day	205.84±09.36	208.16±11.67
14th day	211.36±11.91	213.44±12.75

[a] All values are in mean±SD (n=6, female rats/group)

Table 5.8. Effect of oral administration of compound VA10 on serum concentration of AST, ALT, ALP, and creatinine

Parameters	Normal control [a]	Compound VA10 (300 mg/kg) [a]
AST (U/L)	125.41±8.13	123.56±7.54
ALT (U/L)	38.57±3.37	40.53±3.91
ALP (U/L)	11.28±0.16	10.89±0.17
Creatinine (mg/dL)	0.62±0.048	0.68±0.051
Ck-MB (U/L)	680.11±11.59	674.83±10.92

[a] All values are in mean±SD (n=6, female rats/group), alanine transaminase (ALT), aspartate transaminase (AST), alkaline phosphatase (ALP), creatinine, and creatine kinase- myocardial band (Ck-MD).

5.2.6.2. Scopolamine induced amnesia model

Scopolamine-induced amnesia, most likely caused by a blockade of cholinergic signaling, is used as a pharmacological model of Alzheimer's Disease (AD) [211]. Behavioral studies were conducted to evaluate cognition and memory by scopolamine-induced amnesia model [212]. The effect of compound VA10 (2.5, 5, and 10 mg/kg, p.o) was assessed through a Y maze test, in this cognition improvement was observed by analyzing results of spontaneous alteration behavior in rats (Figure 5.10). The percentage of spontaneous alterations was significantly decreased in the scopolamine control group as compared to normal control group ($P<0.0001$). The percentage of spontaneous alterations was increased in VA10 treated groups (dose-dependent manner) ($P<0.0001$). The potent compound VA10 (10 mg/kg, p.o) treated group showed significant results as compared to DPZ (5 mg/kg, p.o) group ($P<0.0001$). The

behavioral data indicate that administration of VA10 (10 mg/kg) improved cognition and memory in the scopolamine-induced cholinergic deficit.

In addition, compound VA10 effect on neurochemicals (AChE, and ACh) was also estimated in the whole brain of animals. AChE inhibitors decrease the degradation of ACh by blockage of AChE. ACh plays an important role in learning and memory and specifically binds to muscarinic and nicotinic receptors. Increasing central ACh levels can enhance memory ability and comprehensively improve brain function [213]. In VA10 treated groups, AChE levels were decreased in a dose-dependent manner and there is no statistical difference between VA10 (10 mg/kg) and DPZ (5 mg/kg) group ($P<0.0001$) (Figure 5.10). Whereas, scopolamine control group AChE levels were increased as compared to drug-treated groups. The results suggested that compound VA10 (10 mg/kg) successfully inhibited the AChE levels in brain. Furthermore, ACh levels were very low in scopolamine-treated groups as compared to the normal group. In addition, increased ACh levels in VA10 treated groups were observed in a dose-dependent manner (Figure 5.10). The ACh levels were increased in treated rats with VA10 at a dose of 10 mg/kg, these results were significant to DPZ (5 mg/kg) group ($P<0.0001$). These behavioral and neurochemical estimation data suggested that compound VA10 inhibited AChE activity by increasing availability of ACh in the brain.

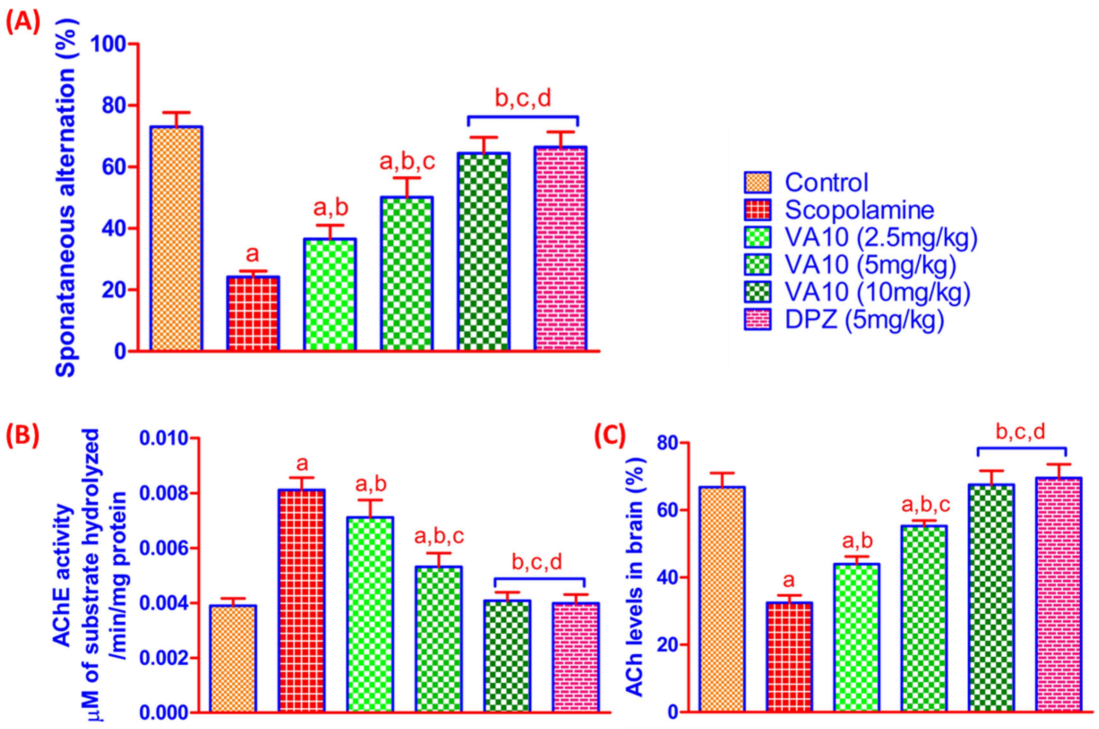

Figure 5.10. Effect of VA10 on scopolamine-induced cognition and memory impairment. (A) showing effect of VA10 on spontaneous alternations (%), (B) showing effect of VA10 on AChE activity in the brain, and (C) showing effect of VA10 on ACh levels in the brain. $^{a}P<0.05$ vs. control; $^{b}P<0.05$ vs. scopolamine; $^{c}P<0.05$ vs. VA10 (2.5 mg/kg); $^{d}P<0.05$ vs. VA10 (5 mg/kg). One-way ANOVA followed by Tukey's post hoc test, n=6.

5.2.6.3. Aβ$_{1-42}$ induced memory deficit rat model

Cerebral aggregation of Aβ$_{1-42}$ is the primary pathological condition in AD. Aβ$_{1-42}$ plaques initiate toxicity and neurodegeneration by activating several biochemical cascades (inflammation, oxidative stress, apoptosis, etc.) resulting in the loss of cognitive and memory function [214]. Cholinergic activity may decrease due to increased AChE activity around amyloid plaques. Previous studies showed that the accumulation of Aβ reduced ACh levels in the AD brain by increasing the expression of AChE [215]. The intracerebroventricular injection (ICV) of Aβ$_{1-42}$ into the rat brain mimics the AD likes behavior, which is similar to human AD

[195]. The $A\beta_{1-42}$ deposits cause neuronal inflammation and microglial activation, which can leads to learning and memory deficits in rats [214].

The learning and memory assessments behavioral studies were performed using morris water maze test. During training trials, the mean escape latency time for rats decreased gradually, and $A\beta_{1-42}$ group (negative control) takes more time to find the platform (Figure 5.11). After completion of last training trial, retention of memory was predicted by a special probe trial test, with the removal of the platform. The time spent on the platform and the total no of entries to the platform zone were also assessed. The time spent in the platform zone was greater in the VA10 (10 mg/kg, p.o) treatment group and results were significant to DPZ (5 mg/kg) group ($P<0.0001$) (Figure 5.11). Search accuracy of the VA10 treated animals was assessed by a total number of platform crossings, and it showed no significant difference with the DPZ group ($P<0.0001$). Removal of the platform led the animals to increase the number of entries to the platform zone and time spent in the platform in VA10 group (10 mg/kg, p.o) was significant to DPZ groups ($P<0001$). However, the $A\beta_{1-42}$ group (negative control) has shown less number of entries to the platform and a number of entries to the platform zone (Fig. 9B). These results suggested that VA10 (10 mg/kg, p.o) improved the spatial memory and cognitive abilities in AD rats.

In *ex-vivo* neurochemical analysis, data indicates that $A\beta_{1-42}$ treated rats significantly increased AChE activity ($P<0.0001$), and ACh levels were decreased in negative control group ($P<0.0001$). VA10 (10 mg/kg, p.o) treated groups significantly decreased the AChE activity, and increased ACh levels were significant to DPZ group ($P<0.0001$). The changes in $A\beta_{1-42}$ induced memory deficits, AChE activity, and ACh levels after treatment with VA10 are depicted in Figure 5.11. These morris water maze test and neurochemical estimation data clears

that compound VA10 (10 mg/kg, p.o) inhibited AChE activity by increasing availability of ACh in the brain and also improving learning and memory in rats.

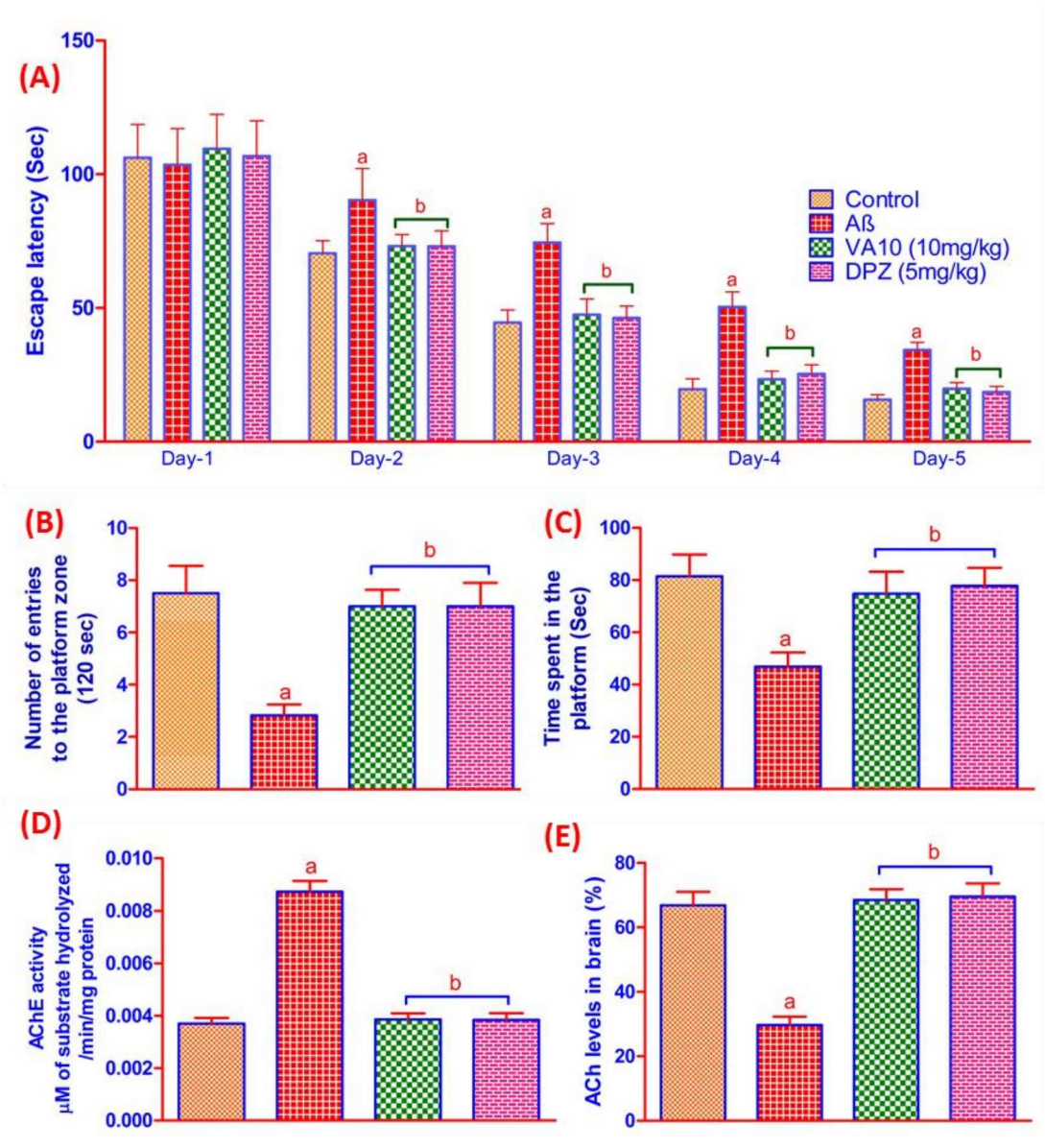

Figure 5.11. Effect of compound VA10 on $A\beta_{1-42}$ induced memory and learning deficits. (A) showing effect of VA10 on escape latency during the training trials, (B) depicts the number of entries to the platform zone, (C) showing animals time spent on the platform during probe trial, (D) showing the effect of VA10 on AChE in the brain, and (E) showing the effect of VA10 on ACh in the brain. $^{a}P<0.05$ vs. normal control, $^{b}P<0.05$ vs. Aβ control. One-way ANOVA followed by Tukey's post hoc test (n=6).

5.2.6.4. Nissl staining

Administration of $A\beta_{1-42}$ by ICV injection in the hippocampus region causes loss of neurons, which results in memory and cognition deficit in the brain [216]. The brain tissue pattern of normal control, $A\beta_{1-42}$ control, VA10 treated group, and DPZ groups were evaluated by histopathological examinations (Figure 5.12). Nissl staining was carried out to identify the morphology of neuronal cells in hippocampus region, which includes DG: dentate gyrus, CA3: cornu ammonis 3, and CA1: cornu ammonis 1 (Figure 5.13) [205]. The normal control group showed that neurons in the hippocampus remain intact and well organized. While, $A\beta_{1-42}$ group (negative control), displayed disordered arrangement of neurons and vascular fibers. Treatment with compound VA10 increased the number of cells (Figure 5.14) and cell density (Figure 5.14) in the hippocampus region (DG, CA3, CA1) and results were significant to normal control/DPZ groups ($P<0.0001$). Degeneration and disordered arrangement of neuronal cells were lowered by treatment compound VA10. These histopathological studies, cell density, and cell number at hippocampus regions suggest that treatment with compound VA10 (10 mg/kg, p.o) restores the neuronal cells and can inhibit neuronal toxicity in AD conditions.

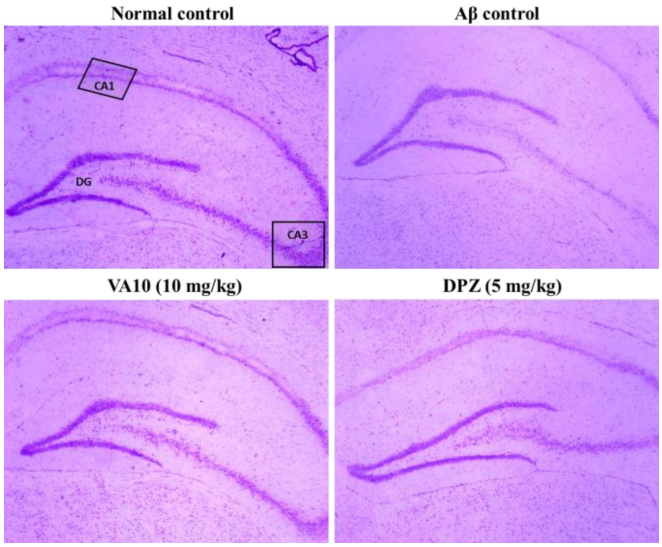

Figure 5.12. Effect of VA10 on $A\beta_{1-42}$ induced neurotoxicity in rats at hippocampal region. Nissl staining, magnification at 4X.

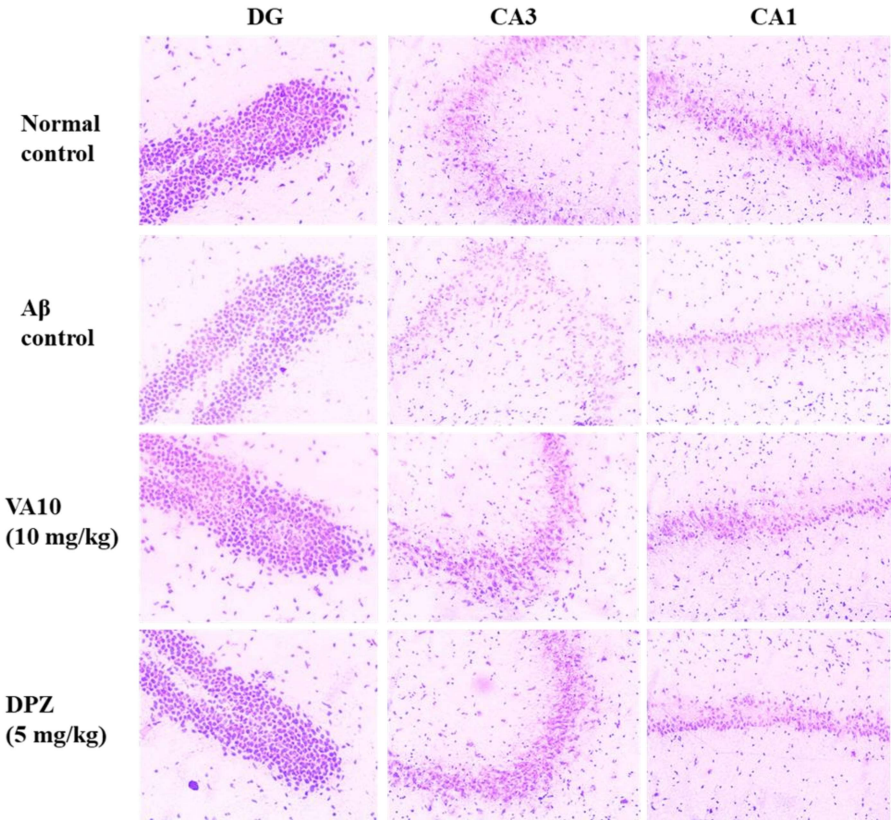

Figure 5.13. The effect of VA10 on $A\beta_{1-42}$ induced neurotoxicity in rats, it indicates the neuronal cell density in hippocampus regions. DG: dentate gyrus, CA3: cornu ammonis 3, and CA1: cornu ammonis 1 respectively. Nissl staining, magnification at 10X.

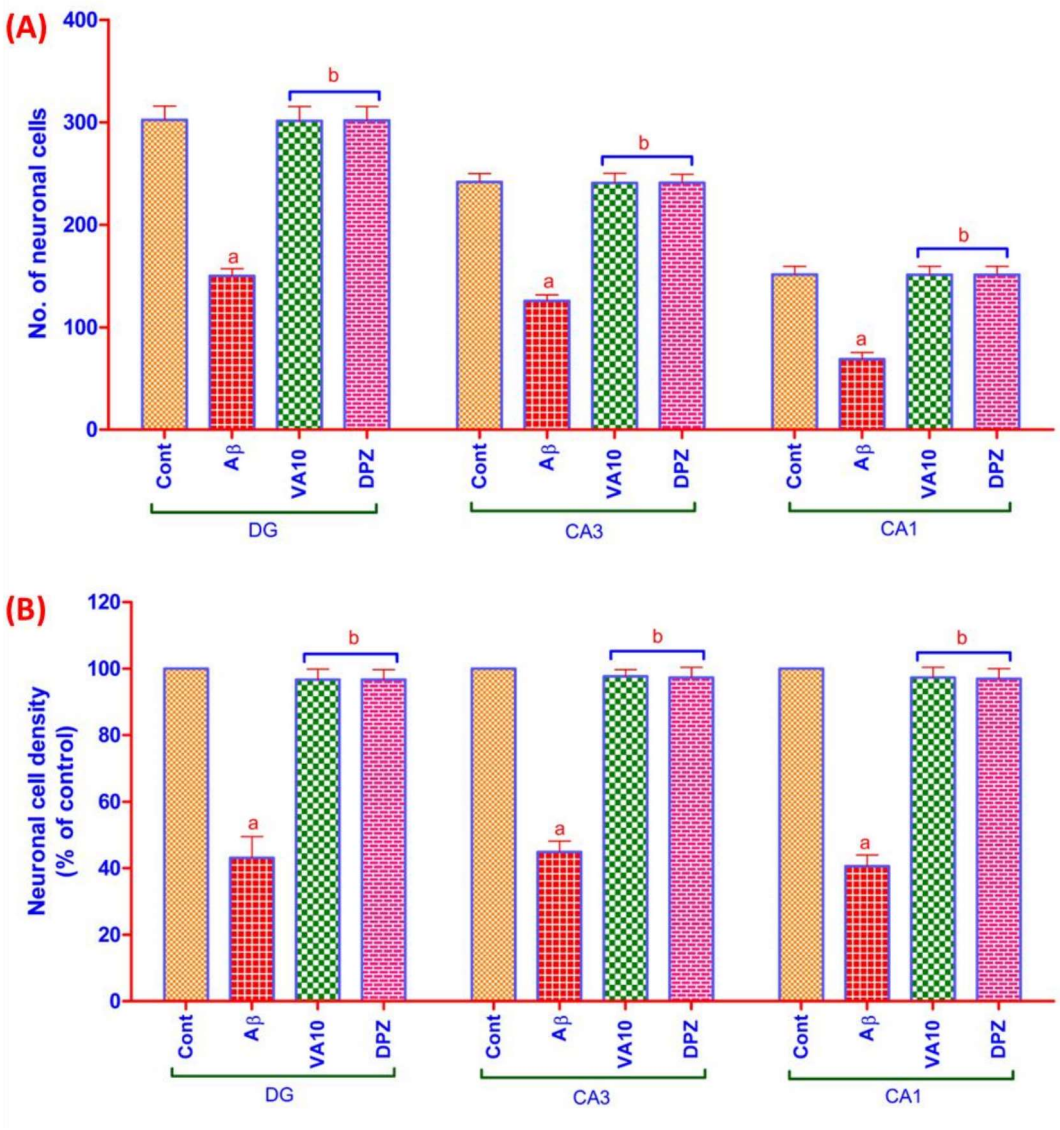

Figure 5.14. Effect of VA10 on $A\beta_{1-42}$ induced neurotoxicity in rats (A) showing the number of neuronal cells and (B) showing neuronal cell density (% of control). $^{a}P<0.05$ vs. normal control, $^{b}P<0.05$ vs. $A\beta_{1-42}$ control. One-way ANOVA followed by Tukey's posthoc test (n=6).

5.3. Conclusion

In summary, multifunctional 3-OH pyrrolidine analogs (VA01-VA25) were prepared through a semisynthetic approach using pyrroloquinazoline alkaloid vasicine as a precursor compound. The current study reports VA10 is a potential molecule among all the synthesized derivatives, which was identified through *in silico*, *in vitro*, and *in vivo* studies. All the compounds exhibited drug-likeness properties, no toxic effects as well as positive ADME profile in *in silico*

predictions as per swissADME and preADMET tools. The preliminary data from *in silico* studies, compound VA10 showed most stable interactions and well resided at AChE and BuChE active sites. Further, compound inhibited the eeAChE, hAChE, eqBuChE, and $A\beta_{1-42}$ aggregation, and showed membrane permeability in PAMPA assay, and anti-oxidant activity in *in vitro* studies. In addition, compound specifically binds to AChE PAS site, as confirmed by propidium iodide displacement assay. Moreover, Compound VA10 showed neuroprotection properties on $A\beta_{1-42}$ treated SH-SY5Y cell line. These *in silico* and *in vitro* experimental data suggested that compound VA10 exhibit drug-like properties and acts via multiple targets i.e. exhibiting cholinesterases inhibition potency by binding to PAS site, inhibiting AChE-induced Aβ aggregation by binding to AChE active site, probably exerting antioxidant activity through free radical scavenging potency by transferring hydrogen atoms to their substrates, PAMPA assay permeability, and neuroprotective action on $A\beta_{1-42}$ treated human neuroblastoma cell line (SH-SY5Y).

Before performing *in-vivo* studies, an acute oral toxicity test was conducted to assess toxicity of novel compound VA10 and it was found to be safe in rats. Further, *in-vivo* screening of hit compound VA10 was performed in AD rat model. Scopolamine induced amnesia model revealed that VA10 (10 mg/kg, p.o) was able to improve cognition in Y maze test and improving ACh levels by inhibiting AChE activity in rats. It is evident that compound VA10 acts through cholinergic pathway and specifically binds to AChE site. Furthermore, improved learning and memory capacity of VA10 was observed through Morris water maze test in $A\beta_{1-42}$ induced Alzheimer model at a dose of 10 mg/kg (p.o). Ex vivo studies reveal increased ACh levels in brain by inhibiting AChE activity. In addition, histopathological examination suggested that neuronal cell density in the hippocampus region was recovered and demonstrated neuroprotective potential in $A\beta_{1-42}$ induced Alzheimer's model. Thus, it was

concluded compound VA10 improved learning and memory by enhancing ACh levels through AChE inhibition, and also the compound was able to recover the neuronal cell loss. The promising data from the *in silico*, *in vitro,* and *in vivo* experiments allow us to report compound VA10 as a potent semi-synthetic multifunctional lead for the treatment of AD.